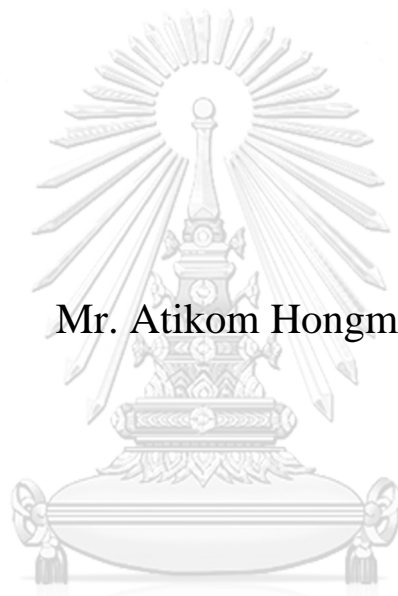


ELECTROLESS CuNiSn ELECTROCATALYST  
SUPPORTED ON CARBON FABRIC FOR  
ELECTROCHEMICAL REDUCTION OF CO<sub>2</sub>



Mr. Atikom Hongmeuan

จุฬาลงกรณ์มหาวิทยาลัย  
CHULALONGKORN UNIVERSITY

A Thesis Submitted in Partial Fulfillment of the Requirements  
for the Degree of Master of Engineering in Chemical Engineering  
Department of Chemical Engineering  
FACULTY OF ENGINEERING  
Chulalongkorn University  
Academic Year 2021  
Copyright of Chulalongkorn University

ตัวเร่งปฏิกิริยาเคมีไฟฟ้าโลหะคอปเปอร์นิกเกิลทินที่ชุบโดยไม่ใช้ไฟฟ้าบนผ้าคาร์บอนสำหรับการ  
รีดักชันด้วยไฟฟ้าเคมีของคาร์บอนไดออกไซด์



วิทยานิพนธ์นี้เป็นส่วนหนึ่งของการศึกษาตามหลักสูตรปริญญาวิศวกรรมศาสตรมหาบัณฑิต  
สาขาวิชาวิศวกรรมเคมี ภาควิชาวิศวกรรมเคมี  
คณะวิศวกรรมศาสตร์ จุฬาลงกรณ์มหาวิทยาลัย  
ปีการศึกษา 2564  
ลิขสิทธิ์ของจุฬาลงกรณ์มหาวิทยาลัย



อติคม หงษ์เหมือน : ตัวเร่งปฏิกิริยาเคมีไฟฟ้าโลหะคอปเปอร์นิกเกิลที่ซบโดยไม่ใช่ไฟฟ้าบนผ้าคาร์บอน  
สำหรับการรีดักชันด้วยไฟฟ้าเคมีของคาร์บอนไดออกไซด์. ( ELECTROLESS CuNiSn  
ELECTROCATALYST SUPPORTED ON CARBON FABRIC FOR  
ELECTROCHEMICAL REDUCTION OF CO<sub>2</sub>) อ.ที่ปรึกษาหลัก : ศ. ดร.จุงใจ ปั้น  
ประณต

ในงานวิจัยนี้ได้ศึกษาการเตรียมตัวเร่งปฏิกิริยาเคมีไฟฟ้าโลหะคอปเปอร์นิกเกิลและทินที่ซบโดยไม่ใช่ไฟฟ้าบนผ้าคาร์บอน ตัวเร่งปฏิกิริยาคอปเปอร์นิกเกิลทินจะถูกนำไปใช้สำหรับการรีดักชันด้วยไฟฟ้าเคมีของคาร์บอนไดออกไซด์ ในเครื่องปฏิกิริยาชนิด H-cell สำหรับผลของเวลาที่ 15 30 และ 45 นาที ในการเตรียมตัวเร่งปฏิกิริยาโลหะผสมไตรเมทัลลิกที่ซบโดยไม่ใช่ไฟฟ้าบนผ้าคาร์บอน ผลลัพธ์นี้แสดงให้เห็นว่าไม่มีความแตกต่างอย่างมีนัยสำคัญสำหรับตัวเร่งปฏิกิริยาทั้งหมดซึ่งแสดงจากเทคนิควิเคราะห์การเลี้ยวเบนของรังสีเอ็กซ์ (XRD) ดังนั้นจึงสรุปได้ว่า เวลาสำหรับการเตรียมตัวเร่งปฏิกิริยาไม่มีผลกับโครงสร้างของตัวเร่งปฏิกิริยา นอกจากนี้การประเมินความสามารถในการรีดักชันด้วยไฟฟ้าเคมีของคาร์บอนไดออกไซด์บนตัวเร่งปฏิกิริยาโลหะผสมไตรเมทัลลิกในช่วงเวลาต่างๆซึ่งถูกตรวจสอบด้วยเทคนิคลิเนียร์สวิตช์โวลแทมเมตรี (LSV) ผลลัพธ์นี้แสดงให้เห็นว่า ตัวเร่งปฏิกิริยาโลหะผสมไตรเมทัลลิกที่ซบโดยไม่ใช่ไฟฟ้าบนผ้าคาร์บอนที่เวลา 30 นาที จะให้ประสิทธิภาพในการเร่งปฏิกิริยาที่สูงกว่าที่เวลา 45 และ 30 นาทีตามลำดับ นอกจากนี้ประสิทธิภาพแบบพาราแคธ และการผลิต H<sub>2</sub> สำหรับโลหะผสมคอปเปอร์นิกเกิลและทิน นั้นต่ำกว่าประสิทธิภาพของตัวเร่งปฏิกิริยาแบบโมนิและไบเมทัลลิก จากผลดังกล่าวแสดงให้เห็นว่าตัวเร่งปฏิกิริยาโลหะผสมไตรเมทัลลิกคอปเปอร์นิกเกิลและทิน มีประสิทธิภาพสำหรับการรีดักชันด้วยไฟฟ้าเคมีของคาร์บอนไดออกไซด์ นอกจากนี้ได้มีการศึกษาการรีดักชันด้วยไฟฟ้าเคมีของคาร์บอนไดออกไซด์ในโลหะผสมคอปเปอร์นิกเกิลและทิน ที่ศักย์ไฟฟ้า -1.6V เทียบกับ Ag/AgCl สำหรับผลิตภัณฑ์ที่อยู่ในรูปของแก๊สถูกตรวจสอบด้วยเทคนิคแก๊สโครมาโทกราฟี (GC) พบว่า H<sub>2</sub> ซึ่งเป็นผลิตภัณฑ์ที่ไม่ต้องการเกิดขึ้นมา สำหรับ โลหะผสมคอปเปอร์นิกเกิลและทิน และโลหะคอปเปอร์ แสดงให้เห็นถึงผลิตภัณฑ์ที่อยู่ในรูปของแก๊ส คือ CO นอกเหนือจาก H<sub>2</sub> เมื่อเทียบกับตัวเร่งปฏิกิริยาอื่นๆ ดังนั้น CO บนโลหะผสมคอปเปอร์นิกเกิลและทิน และ โลหะคอปเปอร์ส่วนใหญ่จึงสามารถส่งผลให้เกิดผลิตภัณฑ์สารประกอบ formate C<sub>2</sub> และ C<sub>3</sub> ได้ จากทั้งหมดที่กล่าวมาข้างต้น งานวิจัยนี้ให้ข้อมูลเชิงลึกใหม่เกี่ยวกับการพัฒนาของตัวเร่งปฏิกิริยาแบบไม่ใช่ไฟฟ้าที่มีราคาต่ำโดยใช้วิธีการซบโดยไม่ใช่ไฟฟ้า

จุฬาลงกรณ์มหาวิทยาลัย  
CHULALONGKORN UNIVERSITY

สาขาวิชา วิศวกรรมเคมี  
ปีการศึกษา 2564

ลายมือชื่อนิสิต .....  
ลายมือชื่อ อ.ที่ปรึกษาหลัก .....

# # 6370318621 : MAJOR CHEMICAL ENGINEERING

KEYWORD Electroless CuNiSn electrocatalyst supported on carbon fabric for  
D: electrochemical reduction of CO<sub>2</sub>

Atikom Hongmeuan : ELECTROLESS CuNiSn ELECTROCATALYST  
SUPPORTED ON CARBON FABRIC FOR ELECTROCHEMICAL  
REDUCTION OF CO<sub>2</sub>. Advisor: Prof. JOONGJAI PANPRANOT, Ph.D.

In the present work, tri-metallic alloy electrocatalysts containing copper (Cu), nickel (Ni), and tin (Sn) supported on Pd-catalyzed carbon fabric substrate were prepared through a simple electroless deposition method. As-deposited Cu-Ni-Sn electrocatalyst was employed in the CO<sub>2</sub>-ERR in an H-cell type reactor. For the effect of electroless deposition time (15, 30 and 45 mins) on tri-metallic alloy electrocatalyst, the result showed that there is no significant difference for all samples based on the XRD pattern, indicating the deposition time had no effect on the crystalline structure of all catalyst. In addition, the evaluation of the ability of the CO<sub>2</sub>-ERR on trimetallic alloy electrocatalyst at different times was investigated using LSV. CuNiSn/CS<sub>30</sub> has a higher catalytic activity than CuNiSn/CS<sub>45</sub> and CuNiSn/CS<sub>15</sub> respectively. Furthermore, the Faradaic efficiency and H<sub>2</sub> production of the Cu-Ni-Sn alloy electrode was lower than that of the monometallic and bimetallic electrocatalysts, suggesting Cu-Ni-Sn alloy electrode was active in the CO<sub>2</sub>-ERR. The CO<sub>2</sub>-ERR using the Cu-Ni-Sn alloy electrode was studied at the applied potential -1.6 V vs. Ag/AgCl. The gaseous products were analyzed by gas chromatography (GC) but an undesired by-product, hydrogen was also produced. For, CuSn/CS<sub>30</sub> and Cu/CS<sub>30</sub> produce gas products with CO other than H<sub>2</sub> compared to other electrocatalysts. Thus, most of CO on CuSn/CS<sub>30</sub> and Cu/CS<sub>30</sub> can be easily converted into formate, C<sub>2</sub> product and C<sub>3</sub> product. Overall, this work provides new insights into the further development of low-cost non-noble electrocatalysts by a simple electroless deposition method.

จุฬาลงกรณ์มหาวิทยาลัย  
CHULALONGKORN UNIVERSITY

Field of Study: Chemical Engineering

Student's Signature

Academic Year: 2021

Advisor's Signature

Year:

.....

## ACKNOWLEDGEMENTS

I would like to thank our advisors : Prof. Dr. Joongjai Panpranot and Dr, Wasu Chaitree for supporting, suggestions and encouragement throughout the planning of this thesis.

They have provided advice, counselling, assistance, and motivation for my thesis since start to first study until last semester to prepare thesis's defense exam, Besides, I am appreciative to Asst. Prof. Dr. Nattaporn tonanon, as the chairman, Asst. Prof. Dr. Suphot Phatanasri and Assoc. Prof. Dr. Okorn Mekasuwandumrong as an examiner of the committee group for their significant guidance and recommendation on this thesis.

Moreover, I am impressed to my parents and my friends for give me a helpful and many valuable suggestions when I faced with stress and many problems.

This research is financially supported by the Thailand Science Research and Innovation (TSRI) National Science, Research and Innovation Fund (NSRF) (Fiscal Year 2022) and the National Research Council of Thailand (NRCT).

Atikom Hongmeuan

# TABLE OF CONTENTS

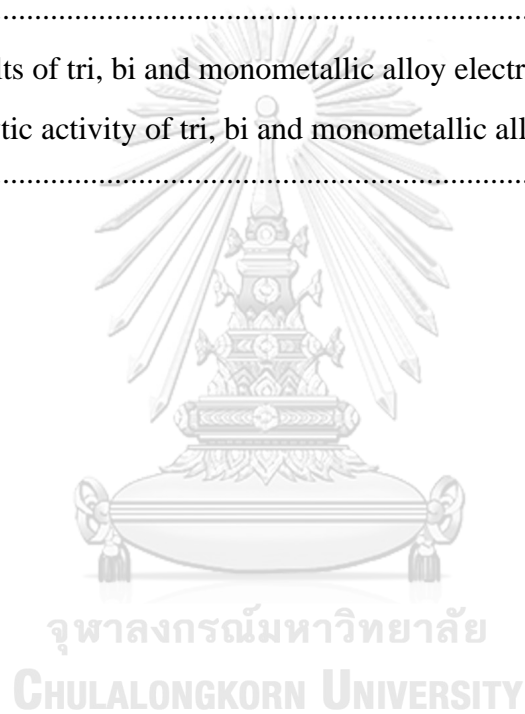
	<b>Page</b>
ABSTRACT (THAI) .....	iii
ABSTRACT (ENGLISH).....	iv
ACKNOWLEDGEMENTS .....	v
TABLE OF CONTENTS.....	vi
LIST OF TABLES .....	1
LIST OF FIGURES .....	2
CHAPTER I.....	3
INTRODUCTION .....	3
1.1 Introduction .....	3
1.2 Objectives of the Research .....	6
1.3 Scope of the Research .....	6
1.4 Expected results .....	7
CHAPTER II.....	8
BACKGROUND AND LITERAURE REVIEWS.....	8
2.1 Electrochemical reduction reaction of CO <sub>2</sub> (CO <sub>2</sub> -RR).....	8
2.2 Fundamental for CO <sub>2</sub> -RR .....	10
2.3 Study on Electrodes .....	13
2.4 Electroless deposition .....	15
CHAPTER III .....	19
MATERIALS AND METHODS.....	19
3.1 Materials .....	19
3.2 Catalyst preparation .....	20
3.2.1 Preparation of Pd-polymer ink. ....	20
3.2.2 Preparation of the Electrocatalysts.....	21
3.3 Catalyst Characterization.....	21

3.3.2 X-ray diffraction (XRD).....	21
3.3.3 Linear sweep voltammetry (LSV).....	21
3.4 Electrochemical reduction reaction of CO <sub>2</sub> (CO <sub>2</sub> -RR) .....	22
3.5 Products analysis .....	23
3.6 Research methodology.....	24
CHAPTER IV .....	27
RESULTS AND DISCUSSION .....	27
4.1 Effect of electroless deposition time on the tri-metallic alloy electrocatalyst...27	
4.1.1 X-ray diffraction (XRD) of CuNiSn/CS electrocatalysts.....	27
4.1.2 Electrochemical reduction reaction of electrocatalysts of CO <sub>2</sub> .....	28
4.2 Characteristic of tri, bi and monometallic alloy electrocatalyst .....	30
4.2.1 Scanning electron microscope-energy dispersive X-ray spectroscopy (SEM-EDX) of electrocatalyst .....	30
4.2.2 X-ray diffraction (XRD) of electrocatalyst .....	35
4.2.3 Electrochemical reduction reaction of electrocatalysts of CO <sub>2</sub> .....	40
4.2.4 Activity test of electrocatalyst for the CO <sub>2</sub> -ERR .....	44
4.3 Stability of electrocatalysts.....	46
CHAPTER V .....	47
CONCLUSIONS.....	47
5.1 Conclusion .....	47
5.2 Recommendations.....	48
REFERENCES .....	49
VITA.....	53



## LIST OF TABLES

	<b>Page</b>
Table 1.CO <sub>2</sub> -RR performed in an H-cell type reactor .....	11
Table 2.The basic elements of any electroless bath and their role are briefly reported .....	15
Table 3.Materials for the preparation of the electroless baths .....	20
Table 4.The operating conditions of gas chromatograph with a thermal conductivity detector.....	23
Table 5.EDX results of tri, bi and monometallic alloy electrocatalyst .....	34
Table 6.The catalytic activity of tri, bi and monometallic alloy electrocatalyst of CO <sub>2</sub> - ERR.....	45



## LIST OF FIGURES

	<b>Page</b>
Figure 1. Carbon Dioxide Conversion Strategies A schematic depicting selected (A) photochemical and photoelectrochemical, (B) biochemical, (C) thermochemical, and (D) electrochemical methods .....	8
Figure 2. Schematics of H-cell .....	10
Figure 3. Possible pathways for CO <sub>2</sub> -RR on metal surfaces in aqueous solution.....	13
Figure 4. Proposed mechanism for carbon dioxide electroreduction. a The pathway to C1 products (formate, carbon monoxide, and methane) and b the pathway to C2 products (ethylene and ethanol) .....	14
Figure 5. CO <sub>2</sub> -RR performed in an H-cell type reactor .....	22
Figure 6. XRD patterns of CuNiSn/CS for deposition time (15, 30, or 45 minutes)....	27
Figure 7. LSV curves of a) CuNiSn/CS_15 b) CuNiSn/CS_30 and c) CuNiSn/CS_45 in N <sub>2</sub> and CO <sub>2</sub> saturated solutions (0.1M KHCO <sub>3</sub> ) with a scan rate 100 mV/s. ....	29
Figure 8. SEM images of (a) CS, (b) CuNiSn/CS, (c) CuSn/CS, (d) CuNi/CS, (e) NiSn/CS, (f) Ni/CS and (g) Cu/CS .....	33
Figure 9. XRD patterns of (a) CS, (b) CuNiSn/CS, (c) CuSn/CS, (d) CuNi/CS, (e) NiSn/CS, (f) Cu/CS and (g) Ni/CS .....	39
Figure 10. LSV curves of a) Carbon fabric b) CuNiSn/CS_30 c) CuSn/CS_30 and d) CuNi/CS_30 e) NiSn/CS_30 f) Cu/CS_30 and g) Ni/CS_30 in N <sub>2</sub> and CO <sub>2</sub> saturated solutions (0.1M KHCO <sub>3</sub> ) with a scan rate 100 mV/s.....	43
Figure 11. Electrochemical stability of electrodes in 0.1M KHCO <sub>3</sub> .....	46

## CHAPTER I

### INTRODUCTION

#### 1.1 Introduction

Due to the mass consumption of fossil fuels, an increasing CO<sub>2</sub> concentration in the atmosphere has posed serious challenges [1], causing a global climate problem as known as “a greenhouse effect”. Therefore, CO<sub>2</sub> reduction reaction (CO<sub>2</sub>-RR) is required to address the global issue of increasing CO<sub>2</sub> emission. To this aim, many researchers have used several approaches to reduce the negative effect related to the increasing CO<sub>2</sub> concentration in the atmosphere including chemical, biological, photochemical, inorganic, and electrochemical methods [1]. Additionally, CO<sub>2</sub>-RR is able to produce energetic compounds [2]–[4]. Among these technologies, CO<sub>2</sub>-RR is an attractive technique because of its features compared with other methods. This reaction can operate at room temperature and atmospheric pressure. In addition, the operational parameters of the reaction (for example, metals, electrolytes, and redox potentials) can be varied to produce various products.

The high-effective electrode is the key factor affecting the performance of CO<sub>2</sub>-RR. Such catalyst must be able to adsorb CO<sub>2</sub> on catalytic surface strongly. Metallic electrodes are classified into 4 types based on their product selectivity : (1) metals that mainly produce HCOOH (Pb, Hg, Cd, In, Sn, and Tl), (2) metals that mainly produce CO (Au, Ag, Pd, Ga, and Zn), (3) metals that form hydrocarbons such as CH<sub>4</sub> and C<sub>2</sub>H<sub>4</sub> (Cu), and (4) metals that mainly produce hydrogen, H<sub>2</sub> (Pt, Ni, Fe, and Ti) [5].

Recently, the CO<sub>2</sub>-RR on modified carbon material electrodes such as glassy carbon electrodes (GCE), graphite, graphene, carbon black, carbon nanotubes (CNTs), carbon fiber and carbon fabric has been investigated. The carbon electrode has distinct properties compared to the metal-based ones, such as extensive lifetime for electrochemical application, relatively low-cost, wider potential window, and controllable surface modification [6]

Carbon fabric is utilized in a variety of industrial applications, including aerospace, electrical equipment, and automobiles. It was also used to make reinforced polymers because it has a lot of good qualities, like high tensile strength and modulus, low density, and good dimension stability [7]. However, the limitations of carbon fabric have been previously focused on its low conductivity and poor wettability in comparison to metals, severely limiting its future applications. To address these issues, metalized carbon textiles with high conductivity have garnered growing scientific interest in the past few years. A variety of methods for metallization have been reported, including electro deposition, chemical vapor deposition, and sputter coating. Most of these methods require expensive equipment and are difficult to scale up. However, this is not the case for the electro deposition. This technique is related to chemical or autocatalytic plating that did not involve external electrical power. In addition, it is cheap and easy to use, and uniform coatings can be made on a wide range of substrates with different shapes and sizes [8].

Solid catalysts have been studied for CO<sub>2</sub>-RR. Copper has also been getting a lot of attention because hydrocarbons, aldehydes, and alcohols have been produced on this metal at high current densities. However, copper electrodes provide low product selectivity due to weak adsorption of CO<sub>2</sub> on catalytic surface. Therefore, copper electrodes have been combined with other non-noble metals (such Ni or Sn). Not only do those metals have low cost, but they favor CO<sub>2</sub> adsorption [9].

For mono-metallic electrodes, Azuma *et al.* [10] reported that the CO<sub>2</sub> reduction efficiency increased dramatically on some metal electrodes (such as Ni) as the temperature decreased. On the other hand, formic acid and carbon monoxide generation in the presence of short and long chain hydrocarbons (methane, ethane, or propane) has been seen on Ni electrodes. When CO<sub>2</sub>-RR was performed on commercial Sn electrode, FE of HCOO<sup>-</sup> production was over 91% in 0.1 M KHCO<sub>3</sub> at - 1.8 V vs. Ag/AgCl [11]. As mentioned earlier, Sn has high selectivity toward HCOO<sup>-</sup>. This phenomenon suggests that the surface oxide of Sn plays an important role in HCOO<sup>-</sup> formation. It has been reported that Sn etched with HBr showed significantly low FE for HCOO<sup>-</sup> production compared with untreated Sn electrode in 0.5 M NaHCO<sub>3</sub> at - 0.7 V vs. RHE [12].

However mono-metallic electrodes show low product selectivity. Recently, multi-metallic electrodes are used for CO<sub>2</sub>-RR because they have multiple active sites able to function during the reaction.

For bimetallic alloy, it could be better for CO<sub>2</sub>-RR performance if Sn or Cu were mixed with another element. This could change the binding energies of reaction intermediates by changing the surface electronic structure of the alloys [13]. For example, Pd-Sn alloy catalysts inhibited the competitive hydrogen evolution reaction (HER) while improving the performance of the CO<sub>2</sub>-RR selectively [14]. Au-Sn alloys exhibited a high Faradaic efficiency for formate [15], and Ag-Sn alloys significantly increased the Faradaic efficiency and current density for formate production when compared to pure Ag or Sn catalysts [16]. In summary, Ke Ye [13] demonstrated a novel strategy for designing a Sn-Cu alloy catalyst using a decorated co-electrodeposition method to achieve high-performance CO<sub>2</sub>-RR to formate conversion. The Sn-Cu alloy is critical in maintaining the devices high Faradaic efficiency and current density when converting CO<sub>2</sub>-RR to formate. With a Faradaic efficiency of 82.3 % at -1.14 V vs. RHE, the Sn-Cu alloy inhibits H<sub>2</sub> and CO evolution and promotes formate production.

Additionally, Xiaolong Zhang [17] studies a coordination enabled galvanic replacement method to decorate atomic Ni clusters on defect-rich Cu surface to provide the first Ni/Cu bimetallic system that significantly enhances the production of C<sub>2</sub> products from electrocatalytic CO<sub>2</sub> reduction. They were found an optimum condition with a surface Ni/Cu ratio of 0.82 %, a 7-fold increase in the selectivity for C<sub>2</sub> products was found in comparison with pristine Cu. A maximum FE of 62 % for C<sub>2</sub><sup>+</sup> products was obtained at -0.88 V vs. RHE in a flow cell with an alkaline 1.0 M KOH electrolyte. For other research related to CuNi bimetallic, Tomiko M. Suzuki [18] studies electrochemical CO<sub>2</sub> reduction over nanoparticles derived from an oxidized Cu–Ni intermetallic alloy. They were found the activated catalyst consists of metallic Cu, Cu–O, Ni, and Ni–O species, as confirmed by XAFS. The product selectivity was highly dependent on the initial Ni composition, and the faradaic efficiency for C<sub>2</sub>H<sub>4</sub> and C<sub>2</sub>H<sub>5</sub>OH production was improved by the addition of a few percent of Ni.

For trimetallic alloy, Tran-Van Phuc [19] studies the Pd, Cu, and Zn trimetallic metal-organic framework electrocatalysts (PCZs) based on benzene-1,3,5-tricarboxylic

were synthesized using a simple solvothermal synthesis. They were found the as-synthesized PCZ catalysts exhibited as much as 95% faradaic efficiency towards CO, with a high current density, low onset potential, and excellent long-term stability during the electrocatalytic reduction of CO<sub>2</sub>.

In this study, the main goal was to demonstrate the feasibility of using a trimetallic composition (Cu, Ni, and Sn) on a carbon fabric through the electroless deposition method for reducing carbon dioxide electrochemically. The effect of deposition times for the metal deposition (15, 30 and 45 min) was studied. In addition, the reaction performances of the tri-metallic compositions were compared to that of bimetallic and monometallic compositions. Last but not the least, electrochemical stability of the electrocatalysts was determined using chronoamperometry.

## **1.2 Objectives of the Research**

- 1.2.1 To investigate the characteristics and the CO<sub>2</sub>-RR performances of CuNiSn electrocatalysts prepared by a simple electroless deposition method
- 1.2.2 To investigate the effect of electroless deposition time for electrocatalyst
- 1.2.3 To investigate the CO<sub>2</sub>-RR performance of the composition for electrocatalyst
- 1.2.4 To investigate the stability of electrocatalyst

## **1.3 Scope of the Research**

- 1.3.1 CuNiSn electroless plating, the Pd-catalyzed carbon fabric substrate (CCS) was cut and immersed in the electroless bath for deposition time (15, 30, or 45 minutes). For other electrocatalysts (bi- and mono-metallic compositions), the best deposition time was used to prepare the sample.
- 1.3.2 The electrocatalytic activity of the electrocatalyst was measured and analyzed using linear sweep voltametric (LSV) techniques.
- 1.3.3 CO<sub>2</sub>-RR was proceeded under various applied potential (-1.6V vs Ag/AgCl ) for 150 mins.
- 1.3.4 CO<sub>2</sub> flow rate before electrolysis was 100 mL/min to achieve the saturated conditions and CO<sub>2</sub> flow rate during electrolysis was 20 mL/min.
- 1.3.5 The catalysts were characterized by
  - Scanning electron microscope-energy dispersive X-ray spectroscopy (SEM-EDX)
  - X-ray diffraction (XRD)

#### 1.4 Expected results

We expect that our study could be an alternative way to development of non-noble electrocatalysts by a simple electroless deposition method for the electrochemical reduction of CO<sub>2</sub> into higher value chemicals.



## CHAPTER II

### BACKGROUND AND LITERATURE REVIEWS

#### 2.1 Electrochemical reduction reaction of CO<sub>2</sub> (CO<sub>2</sub>-RR)

There has not been an increase in the intensity of natural carbon sinks, which has led to an overall rise in greenhouse gas concentrations in the atmosphere. This has an impact on global climate change, air quality, human health, and energy security [20].

Carbon dioxide (CO<sub>2</sub>) is the primary byproduct of fossil fuel combustion. It comes from both point sources, like fossil fuel-fired power plants, and more diffuse sources, like cars and planes. There were 36.2 billion metric tons of CO<sub>2</sub> released into the air by humans in 2015. This caused the global average temperature to rise by 0.1°C since then.[20].

Researchers and entrepreneurs have been working hard to come up with ways to reduce CO<sub>2</sub> in the atmosphere. There are several ways to reduce CO<sub>2</sub> into valuable products, such as thermochemical reduction, photochemical reduction, biochemical reduction, and electrochemical reduction as shown in Figure 1 shows example of these pathways.

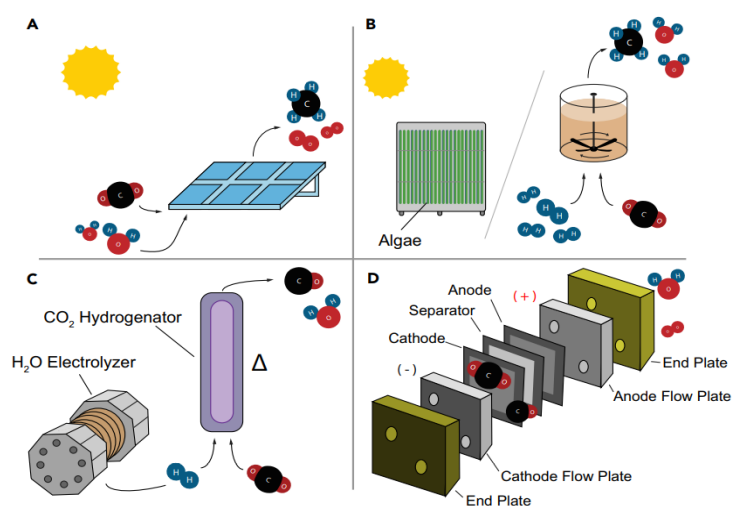


Figure 1. Carbon Dioxide Conversion Strategies A schematic depicting selected (A) photochemical and photoelectrochemical, (B) biochemical, (C) thermochemical, and (D) electrochemical methods [20]



A thermochemical approach may be more advantageous in the long run if there is access to underutilized hydrogen, such as from a chlor-alkali facility [20]. By utilizing solar energy, which is abundant, inexpensive, and ecological, photochemical processes can transform CO<sub>2</sub> into a variety of valuable goods. It's also very expensive, doesn't work very well, and doesn't have a lot of CO<sub>2</sub> affinity, This is a downside to this method [15]. Biochemical reduction of CO<sub>2</sub> involves the production of a specific enzyme by bacteria, algae, or yeast. This enzyme is employed to collect CO<sub>2</sub> and catalyze its reduction to complex compounds. Although this method is environmentally beneficial, it takes a long time to culture bacteria, algae, or yeast and is not stable at high temperatures or pH values [21].

Electrochemical reduction reaction of carbon dioxide (CO<sub>2</sub>-RR) is a cost-effective and ecologically acceptable method of converting CO<sub>2</sub> to a variety of useful chemicals such as hydrocarbon, alcohol, or aldehyde. CO<sub>2</sub>-RR is powered primarily by electricity. CO<sub>2</sub>-RR is an appealing strategy since it offers numerous benefits, including [22].

1. CO<sub>2</sub>-RR can occur at room temperature and pressure.
2. Easy for scale-up application.
3. Electrocatalyst with high selectivity and low cost for the conversion of CO<sub>2</sub> to a variety of valuable compounds in aqueous reaction systems.

## 2.2 Fundamental for CO<sub>2</sub>-RR

A CO<sub>2</sub> molecule is in a linear geometry in which the carbon is attached to each oxygen atom by a double bond. As a result, the adsorption and activation of CO<sub>2</sub> molecules has been thought of as the first step in electrochemical CO<sub>2</sub>-RR. This is because CO<sub>2</sub> molecules bend to weaken the C—O bond by forming chemical interactions with active sites on the surface of electrocatalysts, which bend CO<sub>2</sub> [23].

The electrochemical reduction of CO<sub>2</sub> on a catalyst surface is a multi-step process. First, CO<sub>2</sub> transfers from the gas phase to the bulk electrolyte. The dissolved CO<sub>2</sub> then transports from a bulk electrolyte to the cathode-electrolyte interface and adsorbs at the cathode surface. Following that, the adsorbed CO<sub>2</sub> species dissociate into adsorbed CO<sub>2</sub> and adsorbed CO<sub>2</sub>. \*COOH, \*CO, \*CHO, and \*COH are intermediates. Then, electrons are transferred from the to the from the operating electrode to the intermediates. Finally, the products are ejected from the electrode. Migrate out of the cathode/electrolyte interface and into the bulk gas or liquid phase [24].

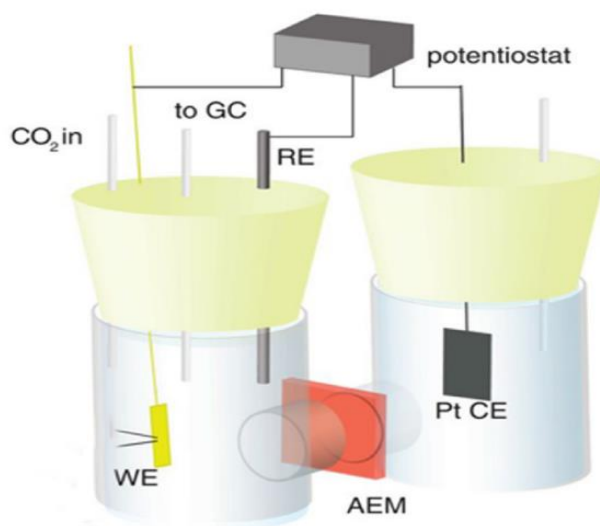


Figure 2. Schematics of H-cell [25].

Currently, the most common CO<sub>2</sub>-RR tool is the H-cell electrolyzer, which can be used in a laboratories and is easy to use [25]. The schematic of an H-cell is shown

in Fig. 2, with the working electrode and reference electrode placed in the cathodic cell and the counter electrode in the anodic cell. A proton exchange membrane separates the cathode and anode to keep products from getting mixed up between them. CO<sub>2</sub> gas flows into the catholyte all the time during the CO<sub>2</sub>-RR process. It is then collected in a gas collecting bag or sent to a gas chromatograph (GC) to detect gas products. Additionally, the liquid products produced by CO<sub>2</sub>-RR are collected from the catholyte and analyzed using nuclear magnetic resonance (NMR) or high-performance liquid chromatography (HPLC), which are processed to produce a variety of products, including carbon monoxide, formate, methane, methanol, and ethylene.

When CO<sub>2</sub>-RR used in electrocatalysis in water, the possible products and their standard redox potentials are shown in Table 1. The standard hydrogen electrode with a pH of 7 at 25°C and a pressure of 1 atm is called E<sub>0</sub>.

Table 1. CO<sub>2</sub>-RR performed in an H-cell type reactor

Reactions	E <sub>0</sub> (V) vs. reversible hydrogen electrode (RHE)
CO <sub>2</sub> + e <sup>-</sup> → CO <sub>2</sub> * <sup>-</sup>	-1.48
2H <sup>+</sup> + 2e <sup>-</sup> → H <sub>2</sub> (g)	0.00
CO <sub>2</sub> + 2H <sup>+</sup> + 2e <sup>-</sup> → HCOOH(l)	-0.19
CO <sub>2</sub> + 2H <sup>+</sup> + 2e <sup>-</sup> → CO(g) + H <sub>2</sub> O	-0.10
CO <sub>2</sub> + 4H <sup>+</sup> + 4e <sup>-</sup> → HCHO(l) + H <sub>2</sub> O	-0.06
CO <sub>2</sub> + 6H <sup>+</sup> + 6e <sup>-</sup> → CH <sub>3</sub> OH(l) + H <sub>2</sub> O	0.03
CO <sub>2</sub> + 8H <sup>+</sup> + 8e <sup>-</sup> → CH <sub>4</sub> (g) + 2H <sub>2</sub> O	0.17
2CO <sub>2</sub> + 12H <sup>+</sup> + 12e <sup>-</sup> → C <sub>2</sub> H <sub>4</sub> (g) + 4H <sub>2</sub> O	0.08
2CO <sub>2</sub> + 12H <sup>+</sup> + 12e <sup>-</sup> → C <sub>2</sub> H <sub>5</sub> OH(l) + 3H <sub>2</sub> O	0.09
2CO <sub>2</sub> + 14H <sup>+</sup> + 14e <sup>-</sup> → C <sub>2</sub> H <sub>6</sub> (g) + 4H <sub>2</sub> O	0.14
3CO <sub>2</sub> + 18H <sup>+</sup> + 18e <sup>-</sup> → C <sub>3</sub> H <sub>7</sub> OH(l) + 5H <sub>2</sub> O	0.10

Parameters used for electro-catalyst performance analysis [23]

### **Onset potential**

The onset potential denotes the point at which the CO<sub>2</sub>-RR begins. Voltammogram data isn't all that is used to figure out the onset potential of CO<sub>2</sub>-RR GC/NMR/HLPC are also used.

### **Total current density**

The total current density is the total number of charges flowing through a unit area of an electrode per unit time, which is used to explain the rate of reaction.

### **Faradaic efficiency**

Faradaic efficiency (FE) represents the selectivity of the desired products in a reaction and can be calculated by using Eq (1)

$$FE = \frac{\alpha n F}{Q} \quad (1)$$

$\alpha$  = the number of transferred electrons

$n$  = the number of mole of a desired product

$F$  = Faraday's constant (96,485 C/mol)

$Q$  = total charge passed during electrolysis

Many factors influence CO<sub>2</sub>-RR product selectivity, including metal electrode type, reactor type, electrolyte, reaction conditions, and electrode surface preparation methods. However, CO<sub>2</sub>-RR is mainly affected by type of metal electrode

### 2.3 Study on Electrodes

The high-effective electrode is the key factor affecting the performance of CO<sub>2</sub>-RR. Such a catalyst must be able to adsorb CO<sub>2</sub> on catalytic surface strongly. Metallic electrodes are classified into 4 group based on their product selectivity. Sn, Pb, Bi, In, Hg, and Cd are included in the first group. These substrates have a difficult time adsorbing the CO<sub>2</sub> intermediate. The molecule then desorbs and undergoes protonation, changing its form to formate or formic acid. The second group of elements, which includes Au, Ag, Zn, Pd, and Ga, readily bind to the CO<sub>2</sub> intermediate. Due to the low adsorption energy of the CO intermediate, this intermediate is further reduced to CO. Pt, Ti, Ni, and Fe are included in the third group. They are selective for the HER due to the fact that these metals were used as inert catalysts for the CO intermediate. As a result, they are not in direct competition with CO<sub>2</sub> reduction. Cu is the only metal that can be used to produce C1-C3 hydrocarbons or alcohols without passing through COH or CHO intermediates [26].

CO<sub>2</sub>-RR has two major pathways, as illustrated in Figure 3. When CO<sub>2</sub><sup>•-</sup> is produced, it reacts with water to form HCOO<sup>•</sup>, which can be reduced to formate (HCOO<sup>-</sup>). As mentioned previously, this pathway is related to the first group. CO<sub>2</sub><sup>•-</sup> is protonated from water in the second route to form <sup>•</sup>COOH. This intermediate undergoes a rapid reduction to CO. This pathway has the potential to occur in the second group. Additionally, the CO intermediate formed on Cu can be converted to hydrocarbons.

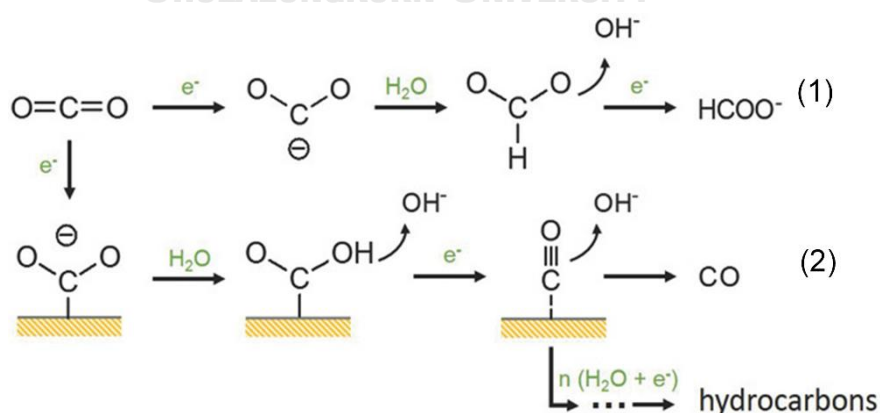


Figure 3. Possible pathways for CO<sub>2</sub>-RR on metal surfaces in aqueous solution [27]

D. Ren et al. [27] proposed the mechanism depicted in Figure 4 for the formation of products over a Cu electrode. The mechanisms can be classified into two distinct pathways: the C1 formation pathway (Fig.4a) and the C2 formation pathway (Fig.4b). The CO intermediate is reduced to either \*OCHO or \*COOH via a proton and an electron transfer in the C1 formation pathway. Following that, \*OCHO or \*COOH is further reduced to HCOO or \*CO. \* Additionally, CO could be converted to CH<sub>4</sub>. In the case of C2 products, \*CO may undergo C-C coupling with another \*CO to produce C2 products such as ethylene (C<sub>2</sub>H<sub>4</sub>) and ethanol (C<sub>2</sub>H<sub>5</sub>OH)

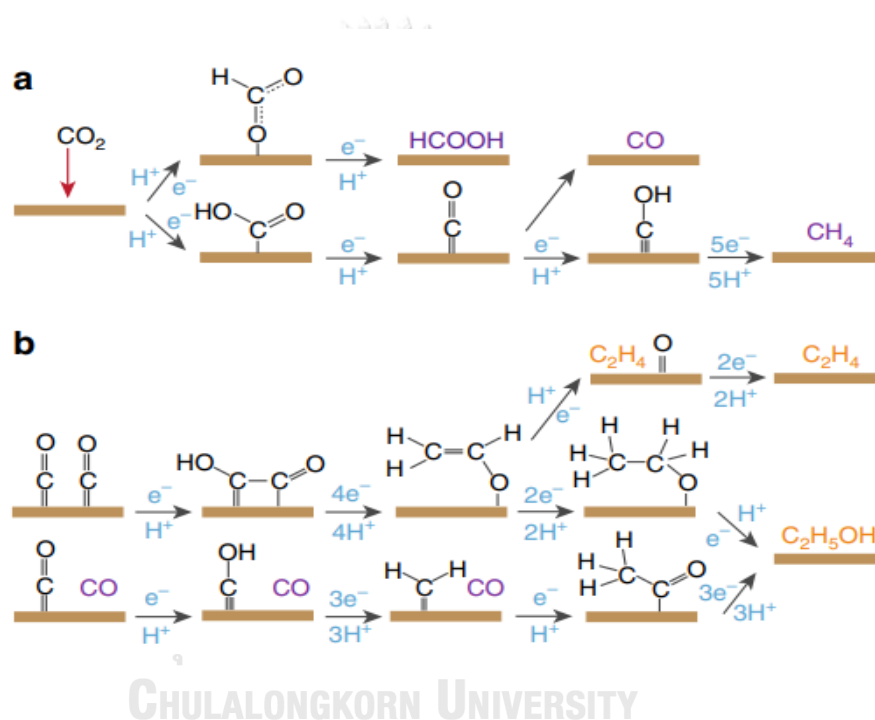


Figure 4. Proposed mechanism for carbon dioxide electroreduction. a The pathway to C1 products (formate, carbon monoxide, and methane) and b the pathway to C2 products (ethylene and ethanol) [28]

## 2.4 Electroless deposition

Electrodeposition utilizes a power source such as a battery or rectifier to electrically charge a component immersed in a chemical solution, altering the chemical composition, and depositing a hard, durable metal coating on the component's surface. Electrodeposition is a more involved process than electroless deposition, requiring clean environments, the use of potentially hazardous equipment, and, in some cases, multiple applications to achieve the desired plating thickness.

Electroless deposition is a chemical or auto-catalytic plating method that occurs without the use of external electrical power. It also has advantages such as low cost and simple handling, and uniform coatings can be obtained on any substrate with various shapes. In a typical electroless deposition process, a metal coating was directly formed on the substrate, which would transform the textile from insulative to conductive.

While the main advantages of electroless plating are uniformity and high quality [8] Electroless deposition is limited by its low deposition rate and the high cost of chemical components in mass production.

Electroless plating solutions contain four main components: (1) the metal ion salt, (2) the pH adjustor, (3) the complexing agent, and (4) the reducing agent. Furthermore, in some recipes, one or more additives are introduced, such as (1) stabilizing agents, (2) brightening agents, and (3) deposition rate-controlling agents [28].

Table 2. The basic elements of any electroless bath and their role are briefly reported

Components	Functions
Metal ions	Source of metal
Reducing agents	Source of electrons to reduce the metal ions
Complexants	Stop excess of free metal ions concentration
Accelerators	Quicken the reducing agent and increase the deposition
Stabilizers	Mitigate the bath from decomposition by protecting catalytically active deposition
Buffers	Endure the pH for long time
pH regulators	pH tuning
Temperature	Energy to the bath deposition

The CO<sub>2</sub>-RR activity of the Cu electrode has attracted attention over the years because it can produce hydrocarbons like methane, ethylene, methanol, and ethanol with a relatively high efficiency. In polycrystalline Cu, CO formation competes with HCOO formation at applied potentials of less than 0.9 V vs. reversible hydrogen electrode (RHE). At 0.9 V, hydrocarbon formation begins with the formation of ethylene, followed by methane. At applied potentials greater than 0.9 V, methane formation takes precedence over ethylene formation, and ethanol, methanol, and C<sub>3</sub> products begin to form. The HER directly competes with the CO<sub>2</sub>RR, but its activity decreases with increasing applied potential [26].

Ni-based alloys and intermetallic offer a unique opportunity to investigate alternatives to Cu-based materials, as Ni is the only other single metal known to reduce CO<sub>2</sub> to C<sub>2</sub> products. Furthermore, Ni has been demonstrated to have the second highest CH<sub>4</sub> yields, albeit at a 0.5 % Faradaic efficiency at extremely low reducing potentials (i.e. less than 1 V vs RHE) [29]. The synthesis of Ni-based intermetallic or alloys should offer the opportunity to modify The reactivity of Ni may possibly improve the activity of Ni for CO<sub>2</sub> reduction.

Sn has been preferably chosen to fabricate copper-based hybrid electrocatalysts due to its high hydrogen evolution overpotential, low cost and non-toxicity [30]. Takanabe *et al.* [31] reported the Cu–Sn bimetallic surface exhibits highly selective and stable performance, resulting in >90% FE toward CO for at least 14 h of CO<sub>2</sub> reduction reaction at –0.6 V vs RHE. A strategy to design selective surfaces is presented, in which the H-binding sites are perturbed to diminish the competitive H<sub>2</sub> evolution without altering the activity toward CO<sub>2</sub> reduction.

Carbon electrodes, including glassy carbon electrodes (GCE), boron doped diamond (BDD), graphite, graphene, carbon black, carbon nanotubes (CNTs), and carbon fabric, have been widely used in electrochemical applications, including electrochemical sensors and electrocatalysis. The carbon electrode has distinct properties compared to the metal-based ones, such as extensive lifetime for electrochemical applications, relatively low cost, wider potential window, and controllable surface modification [6].



Carbon fabric has been used in various industrial fields, such as aerospace, electrical equipment, and automobiles. It has also been used in reinforced polymers because it possesses superior properties such as high tensile strength and modulus, low density, and good dimension [7]. However, the disadvantages of carbon fabric were previously focused on its low conductivity and poor wettability in comparison to metals, severely limiting their future applications. To address these issues, metalized carbon fabrics with high conductivity have garnered increasing research interest in the past few years. Electroless deposition, chemical vapor deposition, and sputter coating are some of the many metallization methods that have been reported [8]. The majority of these methods require expensive equipment and are difficult to scale up.

Fan Liao [32] studied the nickel-coated carbon fabric with continuous and uniform coating was fabricated at 85°C by a simple electroless plating methods. It was found that the nickel-coated carbon fabric composites with compact nickel coating and excellent conductivity were prepared at 85 °C through a facile electroless plating method. The plating parameters, such as the amount of reducing agent used and the reaction temperature, had a significant effect on the quality of the nickel coating and the conductivity of the samples. Increased temperature would provide sufficient energy and accelerate the reaction. However, excessive heat can result in the decomposition of ammonia molecules. The current method was simple and cheap, and it could easily be used to make nickel coatings on other materials.

Reem Y. [33] studied a surface modification and electroless copper (Cu) plating on the carbon fiber (CF) surface. It is also observed that there is no deficiency on the Cu-coated carbon fiber. This is due to the uniform deposit of Cu on the carbon fiber surface by electroless plating.

KARTAL Muhammet [34] synthesis of tin-coated carbon fibers (CFs) by electroless deposition method in aqueous solution was studied. Sn-coated CFs have been successfully synthesized via an electroless deposition method. Could effectively prevent tin particles from aggregation and oxidization. The current approach can be extended to the fabrication of copper coatings on other substrates, and hence it is expected to have various applications in catalysis, sensors, and other fields.

Wasu Chaitree [35] studied Trimetallic electrocatalyst containing Cobalt (Co), Nickel (Ni), and Molybdenum (Mo) was prepared through electroless deposition technique and evaluated for ethanol electro-oxidation. The effects of catalyst composition (correlated to electroless deposition time) and oxidation temperatures (30-60°C) were investigated using an as-deposited Co-Ni-Mo electrocatalyst supported on a Pd-catalyzed carbon substrate (CCS). It was found the trimetallic catalyst showed very low onset potential ( $-0.39$  V vs. Ag/AgCl).



## CHAPTER III

### MATERIALS AND METHODS

#### 3.1 Materials

Chemicals	Grade of purity	Suppliers
1. Palladium (II) Acetate ( $\text{Pd}(\text{OCOCH}_3)_2$ )	98.0%	TCI
2. Polyvinyl Butvral (Butvar B-98)		Eastman Chemical
3. Copper (II) sulfate pentahydrate ( $\text{CuSO}_4 \cdot 5\text{H}_2\text{O}$ )	98.0%	Sigma-Aldrich
4. Nickel (II) sulfate hexahydrate ( $\text{NiSO}_4 \cdot 6\text{H}_2\text{O}$ )	98.0%	Sigma-Aldrich
5. Tin (II) Sulfate ( $\text{SnSO}_4$ )	98.0%	Sigma-Aldrich
6. Potassium sodium tartrate tetrahydrate ( $\text{KOCOCH}(\text{OH})\text{CH}(\text{OH})\text{COONa} \cdot 4\text{H}_2\text{O}$ )	99.0%	Sigma-Aldrich
7. Potassium D-gluconate ( $\text{C}_6\text{H}_{11}\text{KO}_7$ )	99.0%	Alfa aesar
8. Boric acid ( $\text{H}_3\text{BO}_3$ )	99.8%	KemAus
9. Sodium citrate dihydrate ( $\text{HOC}(\text{COONa})(\text{CH}_2\text{COONa})_2 \cdot 2\text{H}_2\text{O}$ )	99.0%	Sigma-Aldrich
10. Sodium hypophosphite monohydrate ( $\text{NaH}_2\text{PO}_2 \cdot \text{H}_2\text{O}$ )	99.0%	KemAus
11. EDTH ( $\text{C}_{10}\text{H}_{16}\text{N}_2\text{O}_8$ )	99.0%	Sigma-Aldrich
12. Formaldehyde	99.0%	Sigma-Aldrich
13. Deionized water		
14. Sodium hydroxide solution	99.0%	Loba Chemie
15. Ethanol solution	99.0%	Sigma-Aldrich
16. Methanol solution	99.0%	Sigma-Aldrich
17. Ammonium hydroxide solution	99.0%	Sigma-Aldrich

### 3.2 Catalyst preparation

#### 3.2.1 Preparation of Pd-polymer ink.

Palladium polymer ink was made by two separate mixtures. First, 0.098 g palladium acetate was mixed with 2 ml  $\text{NH}_4\text{OH}$ . The second mixture was made by dissolving 22 g of polyvinyl Butvral (Butvar B-98) in 140 ml of methanol. Then, the two mixtures were mixed together (approximately 20 h) and stirred until the mixture was well-mixed. The color of the final mixture was light yellow. The catalyst is usually ready to use after 2 hours of stirring, and it can last for up to 10 years in storage.

Table 3. Materials for the preparation of the electroless baths

Chemicals	Electroless baths					
	CuNiSn	CuNi	CuSn	NiSn	Cu	Ni
1. Tin (II) Sulfate	✓		✓	✓		
2. Potassium sodium tetratatrate tetrahydrate	✓	✓	✓	✓	✓	✓
3. Potassium D-gluconate	✓	✓	✓	✓	✓	✓
4. Boric acid	✓	✓	✓	✓	✓	✓
5. Nickel (II) sulfate hexahydrate	✓	✓		✓		✓
6. Sodium citrate dihydrate	✓	✓	✓	✓	✓	✓
7. Copper (II) sulfate pentahydrate	✓	✓	✓		✓	
8. Sodium hypophosphite monohydrate	✓	✓	✓	✓	✓	✓
9. EDTH	✓	✓	✓	✓	✓	✓
10. Formaldehyde	✓	✓	✓		✓	
11. Deionized water	✓	✓	✓	✓	✓	✓

### 3.2.2 Preparation of the Electrocatalysts.

The carbon fabric substrate (CS) from Fuel Cell Earth, AvCarbele, 99.5% was made catalytically active for electroless plating with Pd-polymer ink. Electroless baths were prepared as shown in Table 3

The plating condition was set to a temperature range of 80–85°C and a pH range of 10 – 11 by maintaining pH with NaOH. For CuNiSn electroless plating, the Pd-catalyzed carbon fabric substrate (CCS) was cut and immersed in the electroless bath for a specific time (15, 30, or 45 minutes). After that, DI water and ethanol were used to rinse the plated substrate. The electrocatalyst was then dried overnight at 80°C. CuNiSn/CCS15, CuNiSn/CCS30, and CuNiSn/CCS 45. For other electrocatalysts (bi- and mono-metallic compositions), the best deposition time was used to prepare the sample.

### 3.3 Catalyst Characterization

#### 3.3.1 Scanning electron microscope-energy dispersive X-ray spectroscopy (SEM-EDX)

CuNiSn/CCS, CuNi/CCS, CuSn/CCS, NiSn/CCS, Cu/CCS and Ni/CCS were characterized by scanning electron microscopy (SEM) of Hitachi mode S-3400N and energy dispersive X-ray spectroscopy (EDX) to investigate the morphology of the surface and the bulk composition, respectively.

#### 3.3.2 X-ray diffraction (XRD)

The X-ray diffraction (XRD) pattern of electrocatalyst samples were recorded in the  $2\theta$  range 20°-80° (scan rate = 0.5 sec/step) using a Siemens D5000 diffractometer using nickel filtered Cu  $K_{\alpha}$  radiation.

#### 3.3.3 Linear sweep voltammetry (LSV)

Linear sweep voltammetry is a technique for measuring the current at a working electrode while the potential difference between the working electrode and the reference electrode is swept linearly in time. This method was used to determine the amount of CO<sub>2</sub> reduction that happened as a result of the applied potential. LSV recorded at 10 mVs<sup>-1</sup> and between 0.6 to -1.7 V.

### 3.4 Electrochemical reduction reaction of CO<sub>2</sub> (CO<sub>2</sub>-RR)

The CO<sub>2</sub>-RR was carried out in an H-cell type reactor as shown in Figure 5, and all reaction tests were measured at room temperature and ambient pressure. To separate the anode and cathode compartments and prevent the oxidation of liquid products in the cathode compartment, a Nafion® 117 proton exchange membrane was used. All the reaction tests were directed in a three-electrode cell consisting of the working electrode, the reference electrode (Ag/AgCl), and the counter electrode (Pt foil). The electrocatalyst was used as the working electrodes which were put in electrolyte with a surface area of 1x1 cm<sup>2</sup>. 25 mL of 0.1 M KHCO<sub>3</sub> was used on both sides of the anode and cathode. The electrolyte was saturated with a CO<sub>2</sub> flow rate of 100 mL/min for 60 minutes. After saturated, CO<sub>2</sub> gas was continuously bubbled with flowrate 20 mL/min during the running reaction. Then, the electrolysis was proceeded under constant potential (-1.6V vs Ag/AgCl) for 150 minutes by employing a potentiostat.

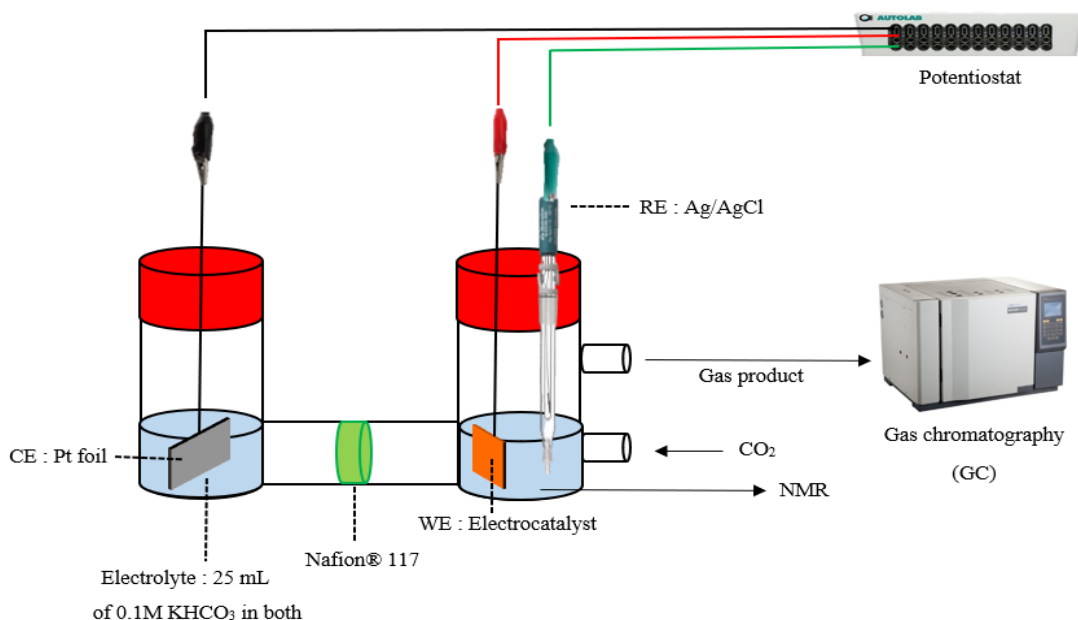


Figure 5. CO<sub>2</sub>-RR performed in an H-cell type reactor

### 3.5 Products analysis

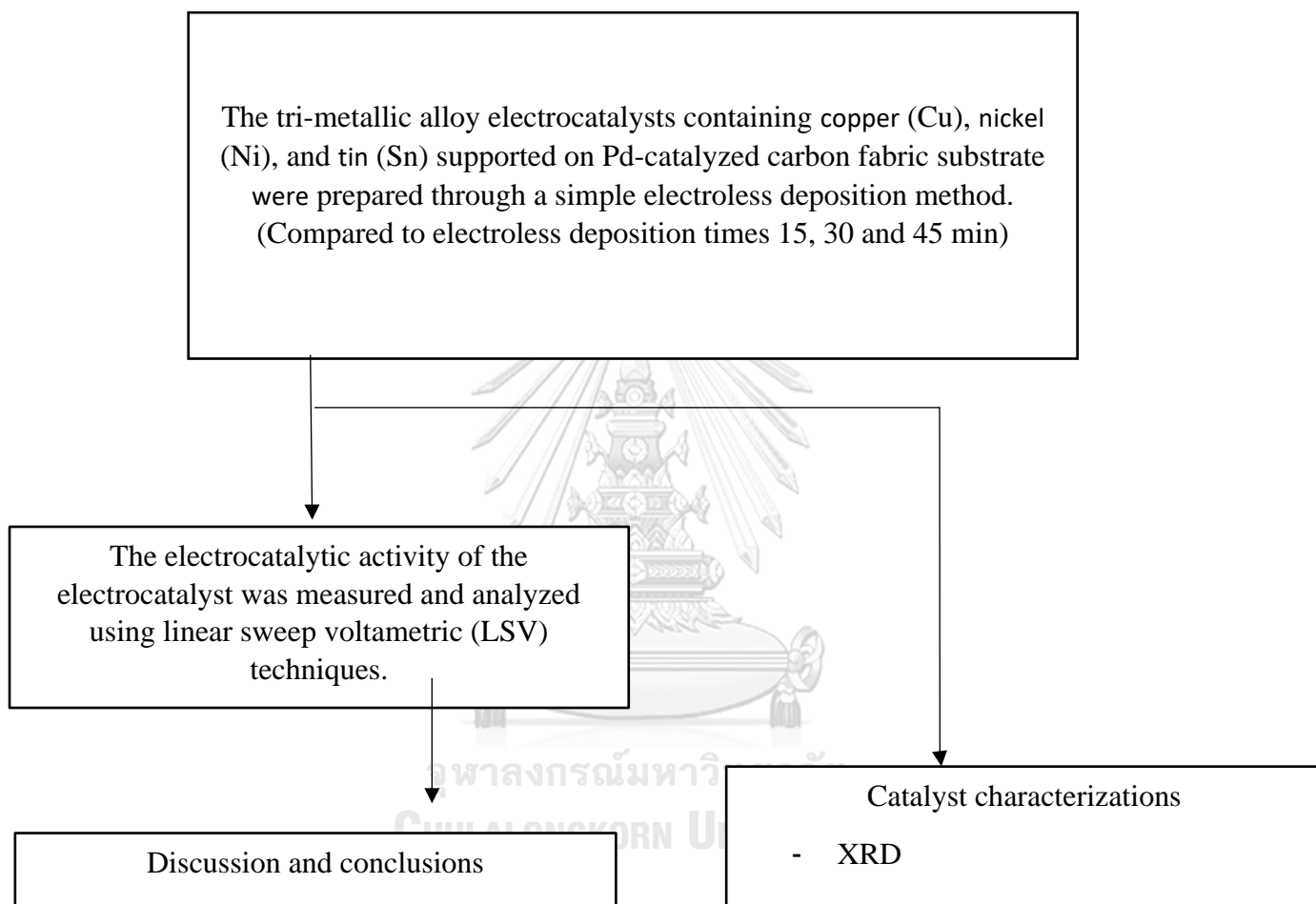
The gas chromatography (GC) system with a thermal conductivity detector (TCD) was used to detect H<sub>2</sub> and CO and the operating condition of GC was shown in Table 4. Liquid phase products were analyzed and quantified using NMR.

Table 4. The operating conditions of gas chromatograph with a thermal conductivity detector

Gas chromatography (Shimadzu GC-2014)	Conditions
Detector	TCD
Column information	Shincarbon ST(50/80)
Carrier gas	Helium (99.999%)
Injector temperature	180°C
Column initial temperature	40°C, Hold time 5 min
Column temperature rate	10°C/min
Column final temperature	200°C
Detector temperature	170°C
Total time analysis	21 min

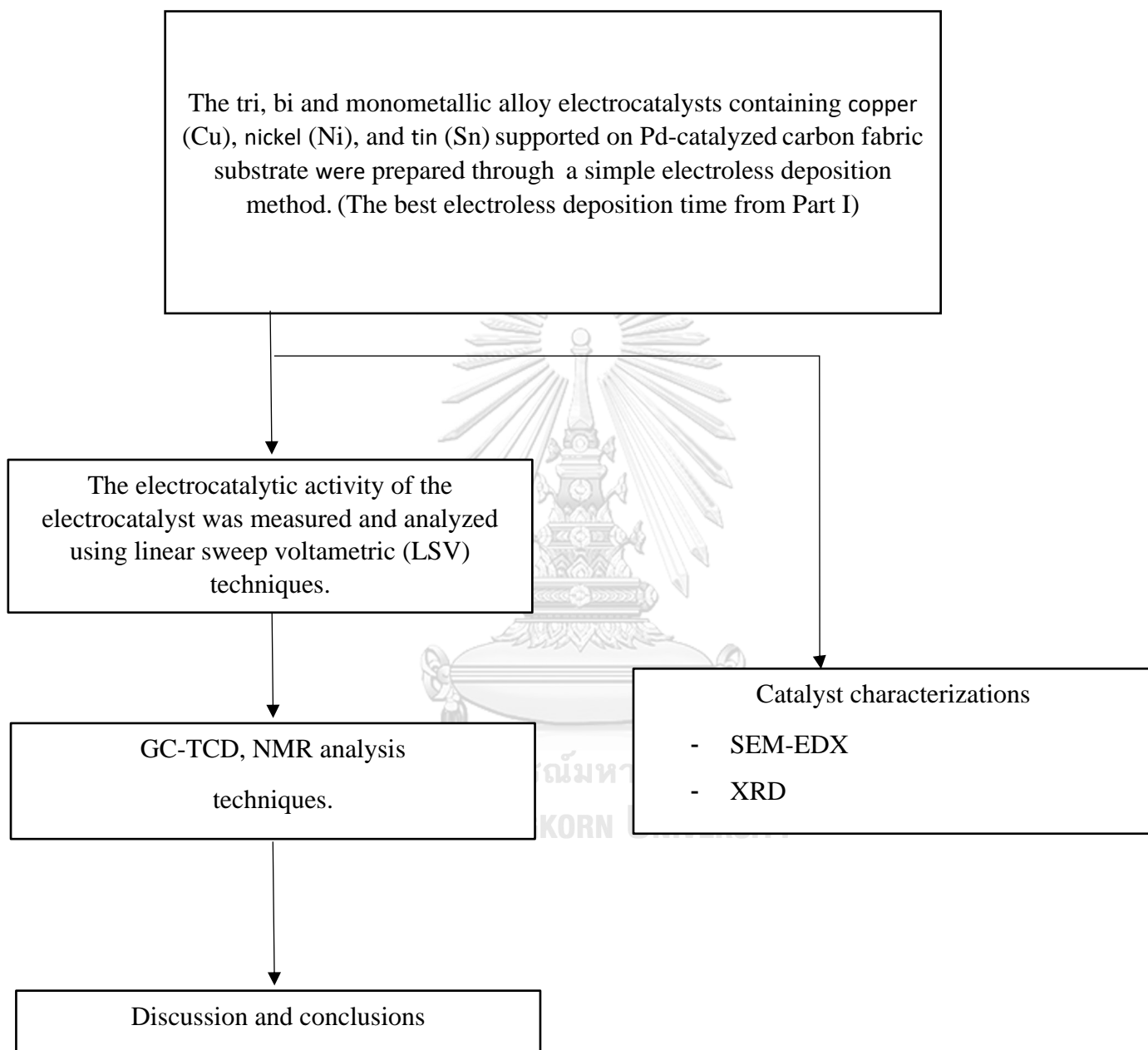
### 3.6 Research methodology

**Part I.** To investigate the effects of electroless deposition time (15, 30 and 45 min) on the tri-metallic alloy electrocatalysts

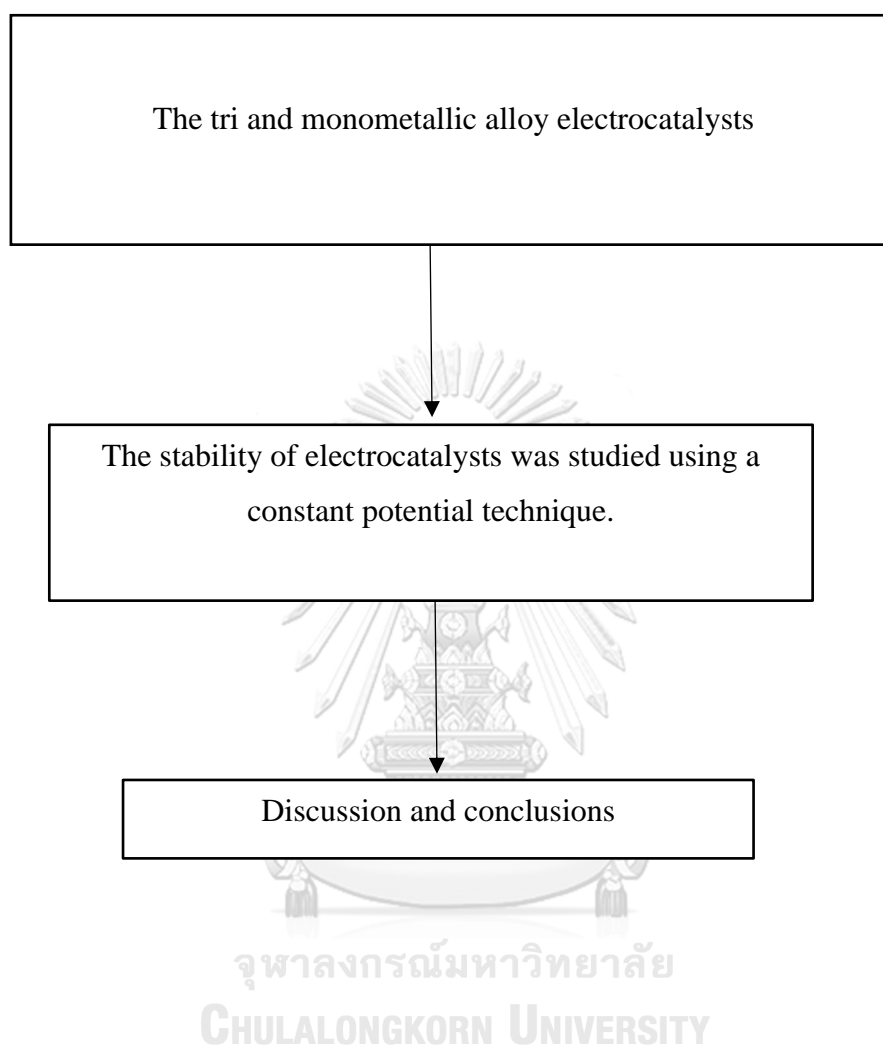




**Part II.** To investigate the characteristic and the electrocatalytic activity of tri, bi and monometallic alloy electrocatalyst



**Part III.** To investigate the activity and stability of electrocatalysts



## CHAPTER IV

### RESULTS AND DISCUSSION

**Part I.** To investigate the effects of electroless deposition time (15, 30 and 45 min) on the tri-metallic alloy electrocatalysts

#### 4.1 Effect of electroless deposition time on the tri-metallic alloy electrocatalyst

##### 4.1.1 X-ray diffraction (XRD) of CuNiSn/CS electrocatalysts

The structure of electrocatalysts were investigated by using X-ray diffraction. Figure 6 shows the crystalline structure of CuNiSn/CS\_15, CuNiSn/CS\_30 and CuNiSn/CS\_45 obtained from electroless deposition of Cu, Ni and Sn on carbon substrate. The result shows that the formation of Cu-Ni was observed at  $2\theta=40^\circ$  and  $50^\circ$ , respectively. In addition, the formation of Ni was also observed at  $2\theta=54^\circ$ . However, the peaks corresponding to tin were not detected probably due to low amount of metal appearance. The XRD result indicates the alloy formation of Cu, Ni, and Sn on the carbon substrate. Furthermore, no significant difference for all samples based on the XRD patterns was observed. Thus, it can be concluded that the deposition time had no effect on the crystalline structure of all catalysts.

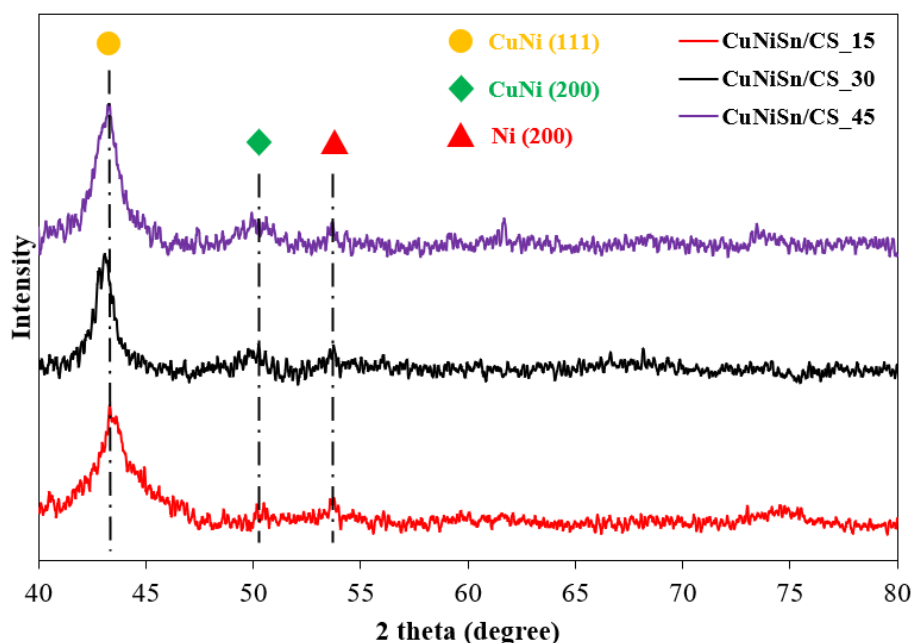
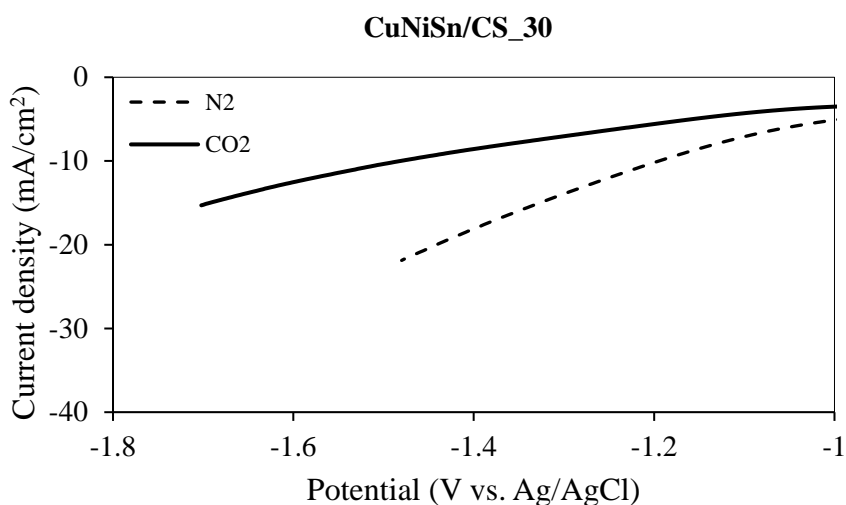
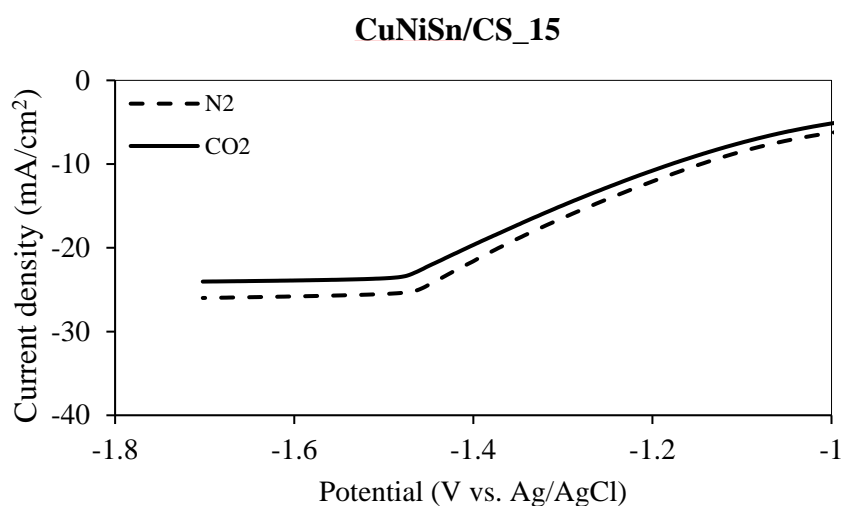


Figure 6. XRD patterns of CuNiSn/CS for deposition time (15, 30, or 45 minutes)

#### 4.1.2 Electrochemical reduction reaction of electrocatalysts of CO<sub>2</sub>

The reaction performances using CuNiSn/CS<sub>15</sub>, CuNiSn/CS<sub>30</sub> and CuNiSn/CS<sub>45</sub> electrocatalyst for the CO<sub>2</sub>-ERR were evaluated. Current curves at the most negative potentials were also monitored in the base electrolyte following 20 minutes of CO<sub>2</sub> saturation.

LSV for the electrocatalysts prepared by electroless deposition method are displayed in Fig.7a-7c. Generally, in absence of CO<sub>2</sub> (dotted curve), the currents below -1.00V vs. Ag/AgCl are associated with hydrogen formation, whereas the signals developed in the base electrolyte following CO<sub>2</sub> saturation (black curves) are associated with both hydrogen evolution reaction (HER) and CO<sub>2</sub> reduction.



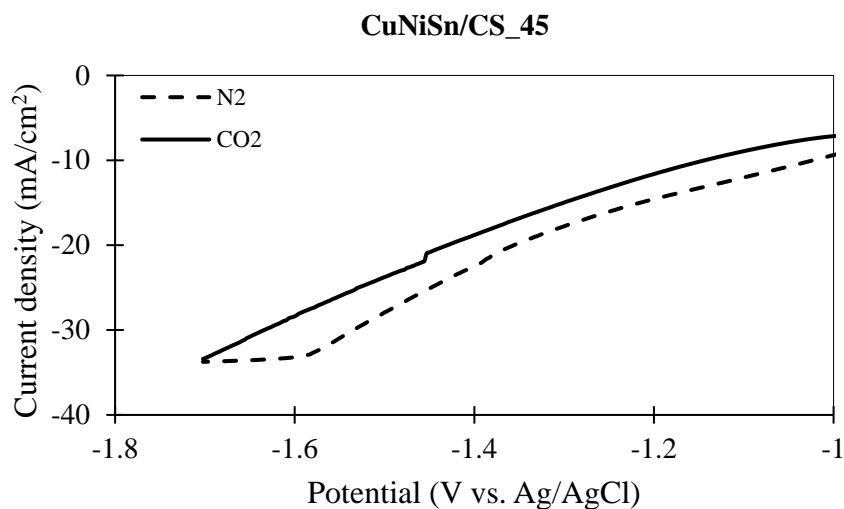


Figure 7. LSV curves of a) CuNiSn/CS\_15 b) CuNiSn/CS\_30 and c) CuNiSn/CS\_45 in N<sub>2</sub> and CO<sub>2</sub> saturated solutions (0.1M KHCO<sub>3</sub>) with a scan rate 100 mV/s.

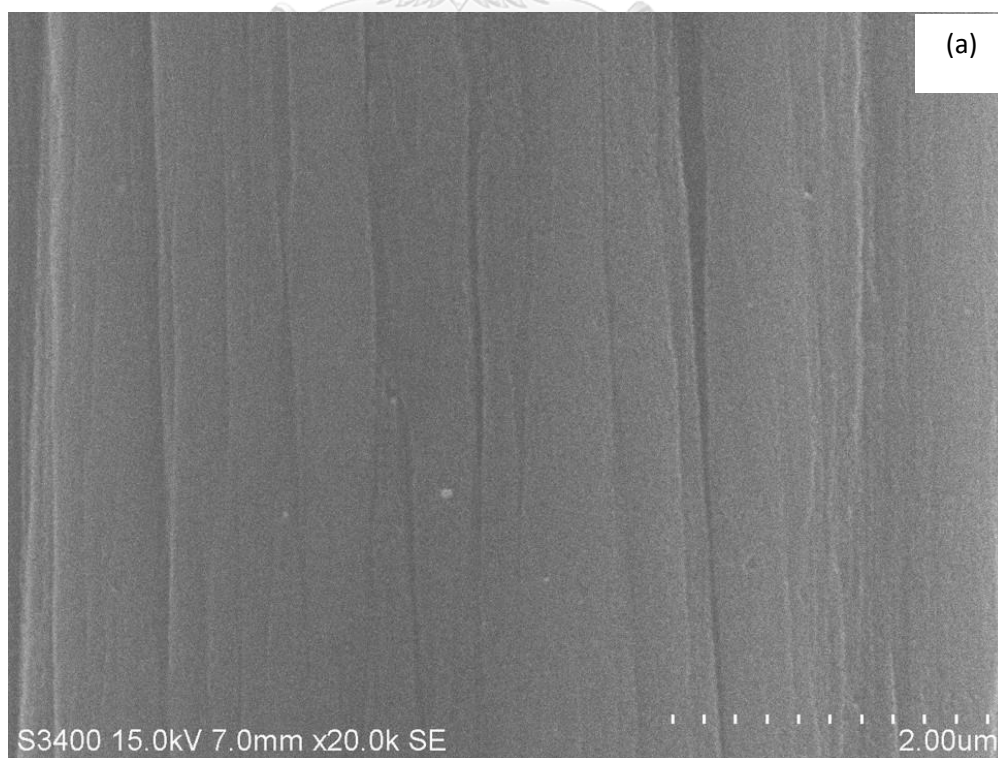
All the tri-metallic alloy electrocatalysts at different deposition times behaved similarly in the presence of CO<sub>2</sub>, the cathodic current was decreased at potentials less than -1.0 V vs. Ag/AgCl, which is attributed to the inhibition of HER due to the adsorption of species derived from CO<sub>2</sub> reduction such as CO and formates [30]. These results show that CO<sub>2</sub> is effectively reduced to adsorbed species on all the catalyst surfaces [9]. In addition, the evaluation of the ability of the CO<sub>2</sub>-ERR on tri-metallic alloy electrocatalysts at different times was investigated using LSV (Figure 7-9). The dotted curve and black curve corresponded to rate of hydrogen evolution reaction (HER) and rate of the CO<sub>2</sub>-ERR respectively. For CuNiSn/CS\_30 in Fig.7b, the gap between these curves, which related to the rate of product, was larger than that for CuNiSn/CS\_15 and CuNiSn/CS\_45 in Fig.7a and Fig.7c respectively. It suggested that CuNiSn/CS\_30 had higher catalytic activity than CuNiSn/CS\_45 and CuNiSn/CS\_15, respectively.

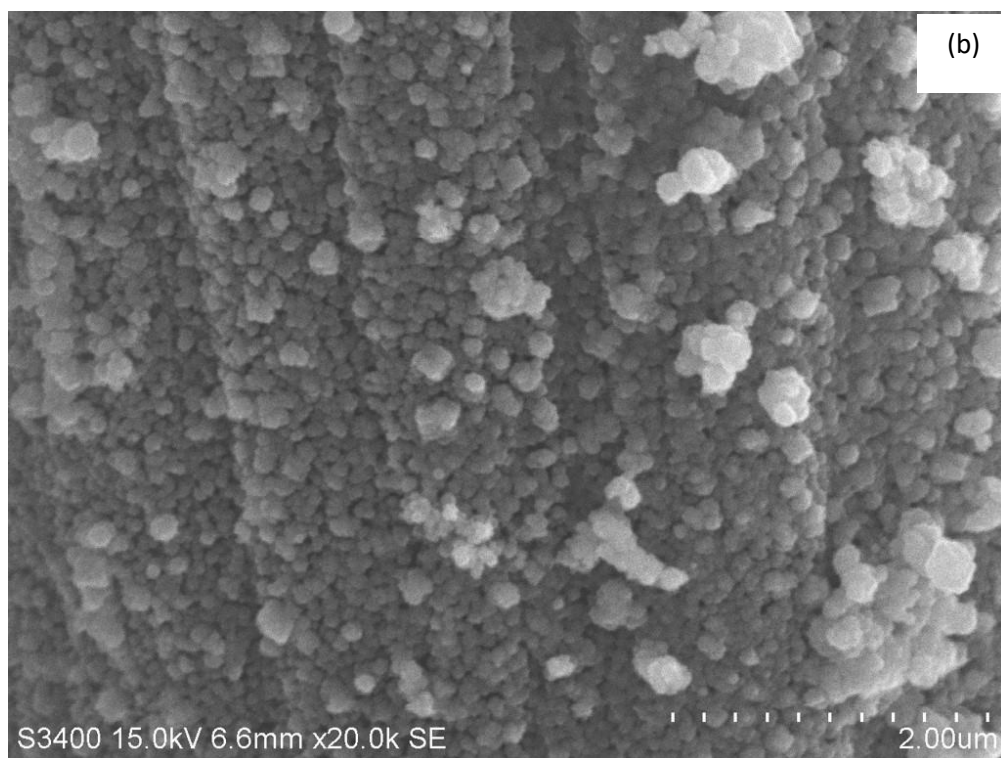
**Part II.** To investigate the characteristic and the electrocatalytic activity of tri, bi and monometallic alloy electrocatalyst

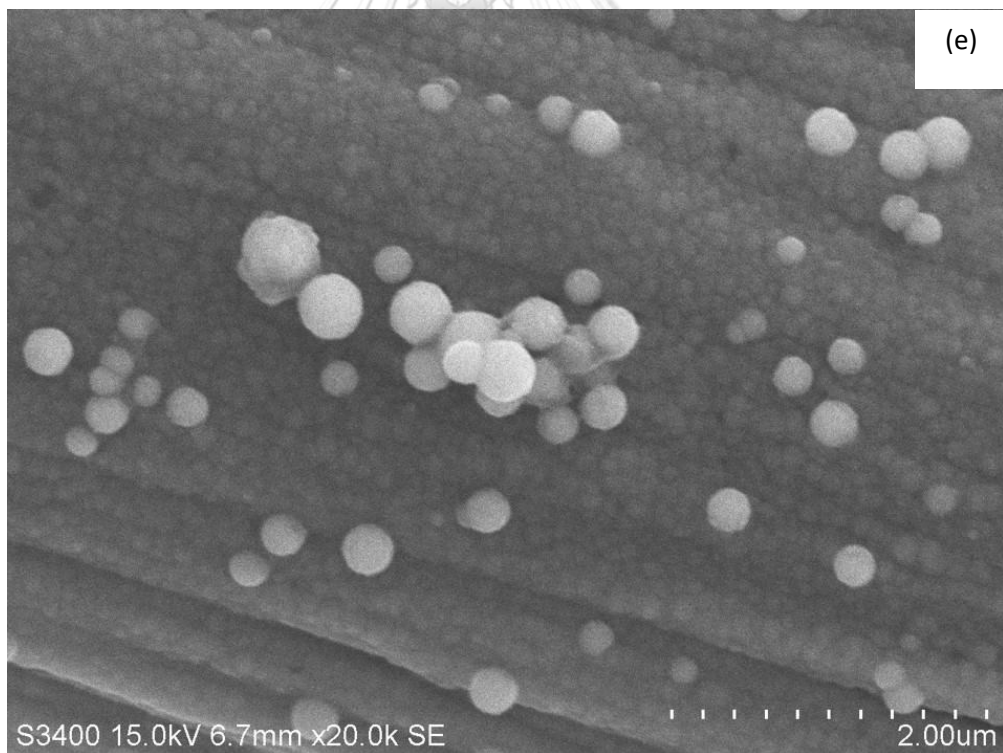
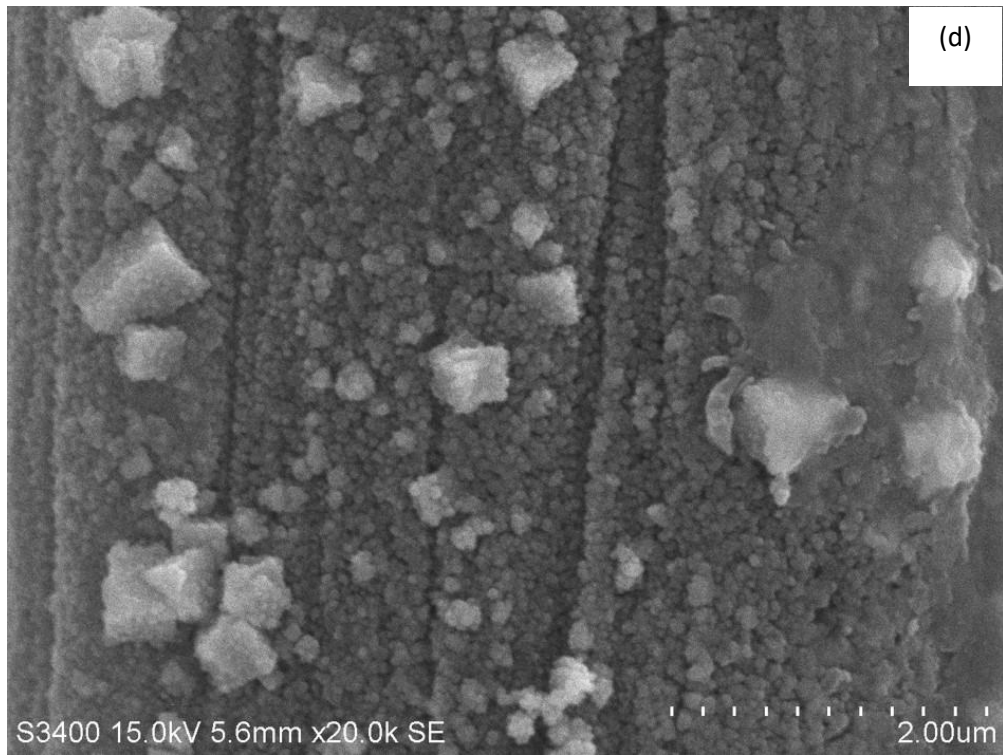
## **4.2 Characteristic of tri, bi and monometallic alloy electrocatalyst**

### **4.2.1 Scanning electron microscope-energy dispersive X-ray spectroscopy (SEM-EDX) of electrocatalyst**

Figures 8a-8d represent SEM images of the electrocatalysts synthesized by electroless deposition method (30 min). A carbon fabric substrate shows clean surface and cylindrical structure (Fig. 8a). For CuNiSn/CS, CuSn/CS, CuNi/CS and Cu/CS electrocatalysts (Fig.8b, 8c, 8d and Fig.8g respectively), the figures show that particles were deposited on the carbon fabric. The images demonstrate that the particles deposited on the surface were spherical and non-uniform. For NiSn/CS and Ni/CS electrocatalysts (Fig.8e and Fig.8f), the nickel layer on the surface of the carbon fabric is uniform and compact, with no observable scattered nickel particles on the coating surface. It indicates that nickel was deposited mainly on the surface of the carbon fabric and not in the reaction solution [32].









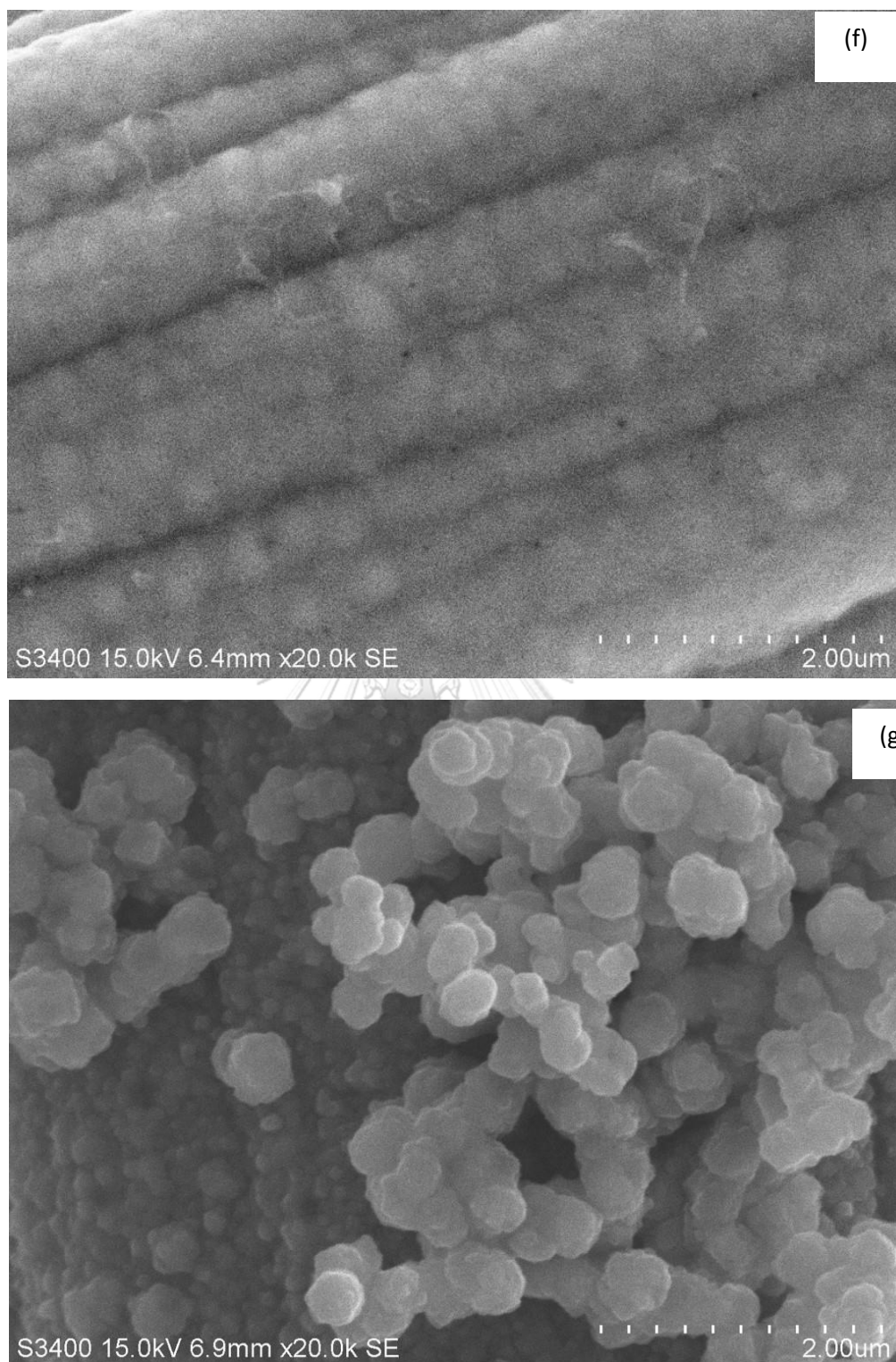


Figure 8. SEM images of (a) CS, (b) CuNiSn/CS, (c) CuSn/CS, (d) CuNi/CS, (e) NiSn/CS, (f) Ni/CS and (g) Cu/CS

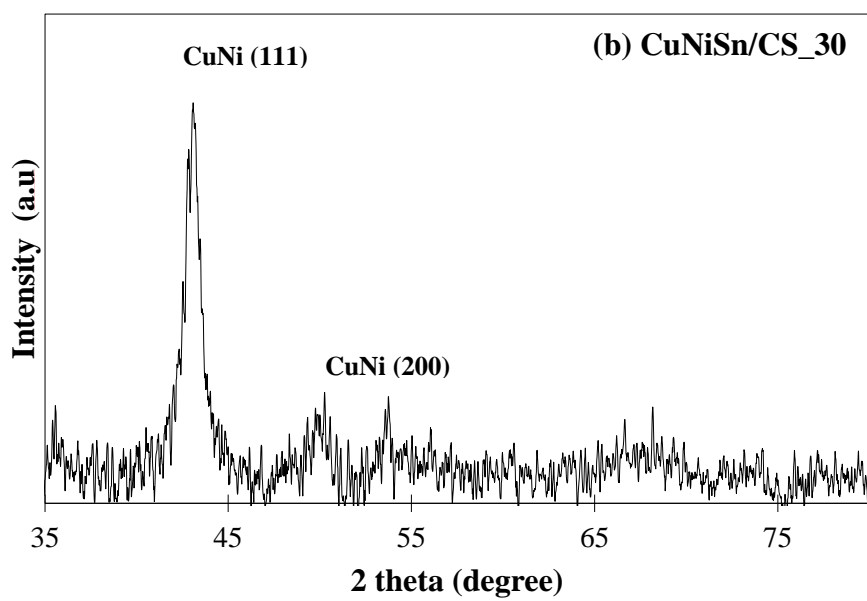
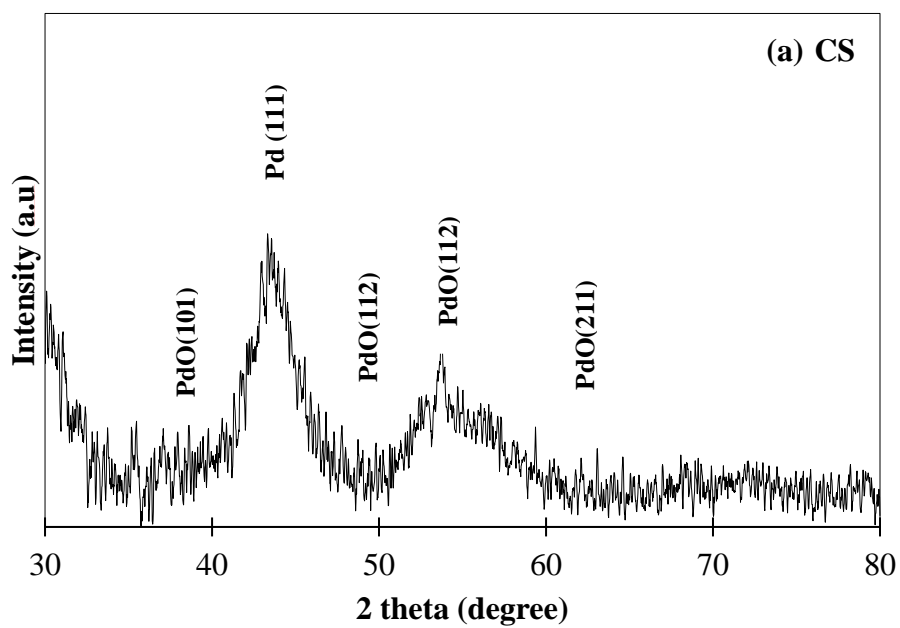
Table 5. EDX results of tri, bi and monometallic alloy electrocatalyst

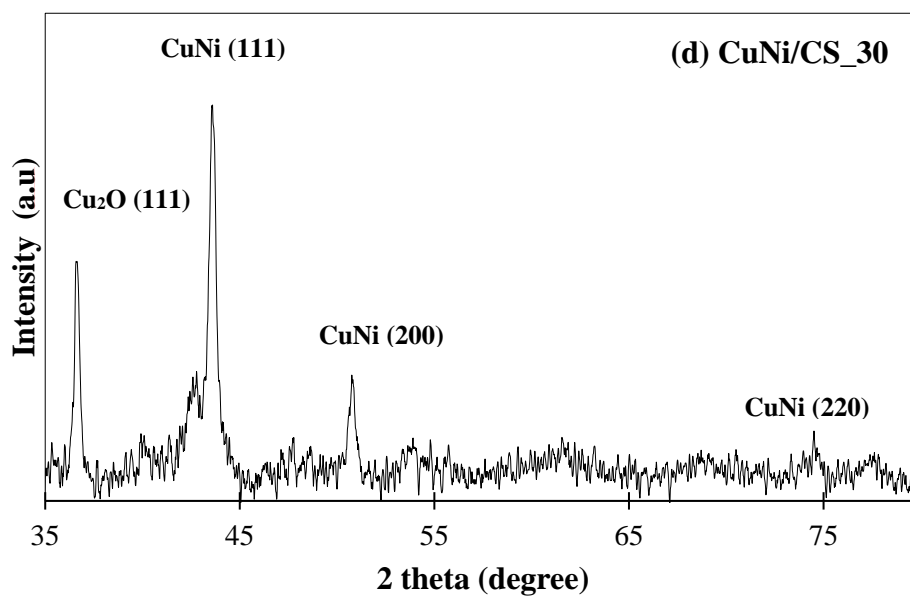
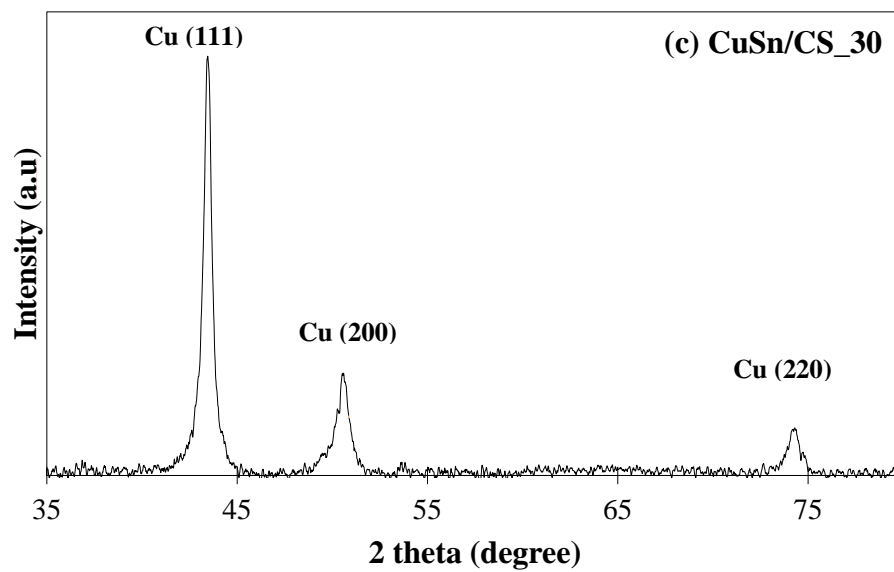
EDX is used to study the elements distribution on the carbon fabric and the result are shown in Table 5. For copper-based electrocatalysts, CuNiSn/CS\_30, CuSn/CS\_30 and CuNi/CS\_30 showed that copper was the main species and small amount of deposited nickel and tin was observed. It is suggested that Cu was reduced by both reducing agents, including sodium hypophosphite monohydrate and formaldehyde, while Ni was reduced by sodium hypophosphite monohydrate only [36]. In addition, the trace amount of added Sn was observed during the electroless deposition preparation. For nickel-based electrocatalysts, nickel was the main species for NiSn/CS\_30 because nickel and tin could be reduced by sodium hypophosphite monohydrate, but the smaller amount of tin precursor ( $\text{SnSO}_4$ ) was used compared to the amount of  $\text{NiSO}_4$ . Finally, for monometallic electrodes, Cu/CS\_30 and Ni/CS\_30 show that the copper and nickel were deposited on the carbon surface, respectively.

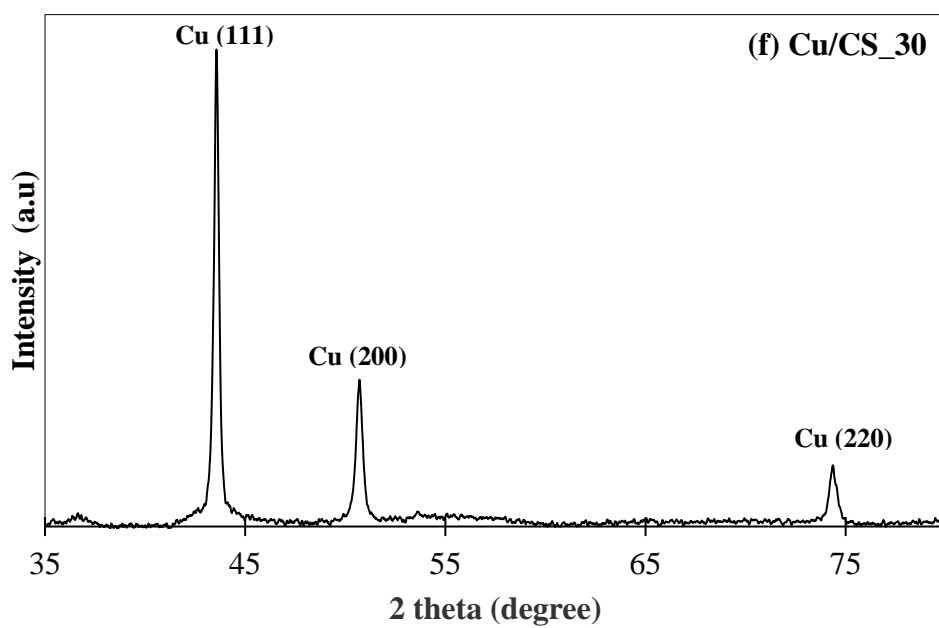
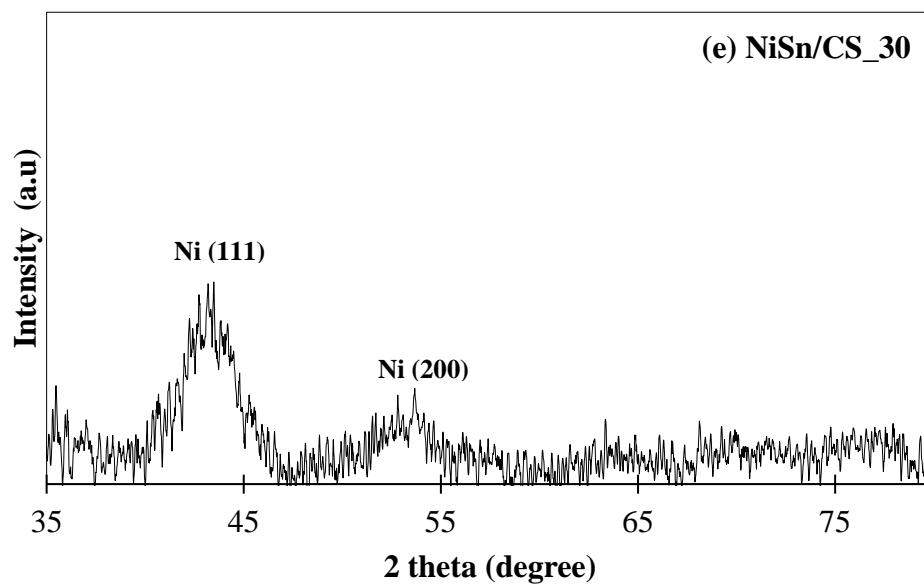
Electrocatalysts	The percent by atom (%)			
	Cu(%)	Ni(%)	Sn(%)	C(%)
1.CuNiSn/CS_30	54.63	11.28	1.40	32.69
2.CuSn/CS_30	88.06	-	0.86	11.08
3.CuNi/CS_30	28.95	3.47	-	67.58
4.NiSn/CS_30	-	39.61	1.23	59.16
5.Cu/CS_30	94.22	-	-	5.78
6.Ni/CS_30	-	49.48	-	50.52

#### 4.2.2 X-ray diffraction (XRD) of electrocatalyst

Next, the electrocatalysts were investigated by using X-ray diffraction (XRD). Figure 9a – 9g shows the crystalline structure. All patterns of electrocatalysts show amorphous phase. The XRD of carbon substrate after catalyzing surface with Pd-polymer ink (Fig.9a), the XRD shows peak at  $2\theta=33^\circ$ ,  $55^\circ$  and  $61^\circ$ , indicating that PdO was formed [35] and peak at  $40.1^\circ$  are attributed to Pd [35]. For tri-metallic alloy electrocatalyst, the CuNiSn/CS\_30 (Fig.9b) that the formation of Cu-Ni was observed at  $2\theta=40^\circ$  and  $50^\circ$ [37] respectively. For bi-metallic alloy electrocatalysts, the CuSn/CS\_30 (Fig.9c) shows sharp peak at  $2\theta=40^\circ$ ,  $50^\circ$  and  $75^\circ$ , indicating that Cu was formed [33]. For CuNi/CS\_30 (Fig.9d) show the formation of Cu-Ni was observed  $2\theta=40^\circ$  and  $50^\circ$  [37] respectively and peak at  $2\theta=36^\circ$  indicating that  $\text{Cu}_2\text{O}$  was formed [38]. The XRD pattern of NiSn/CS\_30 (Fig.9e) shows the peak at  $44^\circ$  and  $54^\circ$ , indicating that Ni are formed [32]. For mono-metallic electrocatalyst, the Cu/CS\_30 (Fig.9f) shows a sharp peak at  $2\theta=40^\circ$ ,  $50^\circ$  and  $75^\circ$ , indicating that Cu was formed [33] which looks like the XRD pattern of CuSn/CS\_30. Finally, the XRD pattern of Ni/CS\_30 (Fig.9g) shows the peak at  $44^\circ$  and  $54^\circ$ , indicating that Ni was formed [32] which was similar to the XRD pattern of NiSn/CS\_30. However, For CuNiSn/CS\_30 (Fig.9b), CuSn/CS\_30 (Fig.9c) and NiSn/CS\_30 (Fig.9e) the peaks corresponding to tin were not detected, probably due to the low amount of metal appearance.







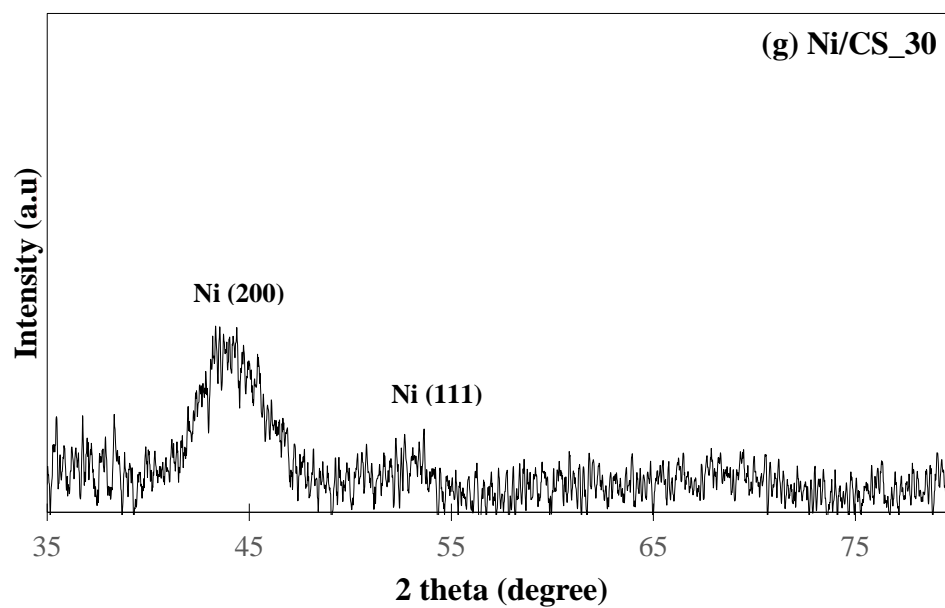
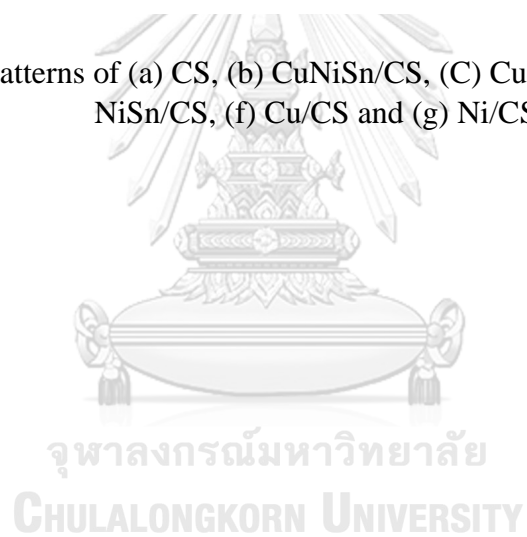


Figure 9. XRD patterns of (a) CS, (b) CuNiSn/CS, (c) CuSn/CS, (d) CuNi/CS, (e) NiSn/CS, (f) Cu/CS and (g) Ni/CS



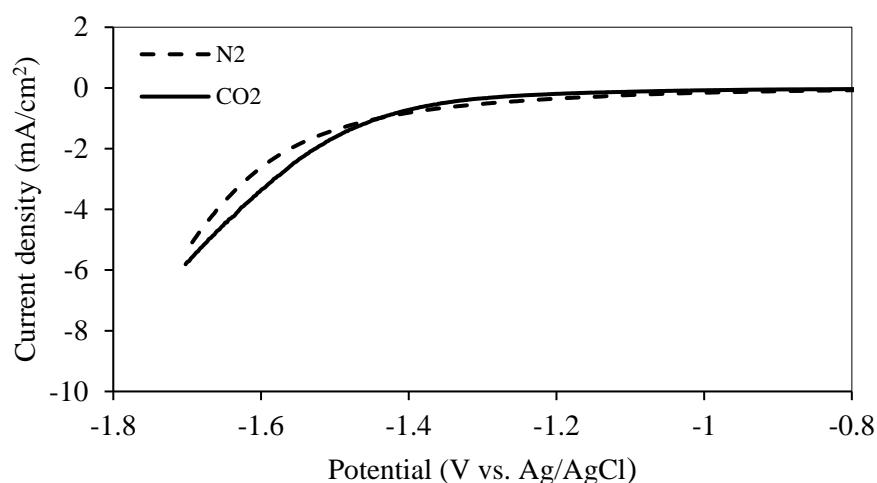
### 4.2.3 Electrochemical reduction reaction of electrocatalysts of CO<sub>2</sub>

To evaluate the ability of the CO<sub>2</sub>-ERR on carbon fabric and tri, bi and monometallic alloy electrocatalysts prepared by electroless deposition method at 30 minutes, linear sweep voltammetry (LSV) was applied under N<sub>2</sub> and CO<sub>2</sub> saturated solution. As shown in Figure 10a. – 10g., dotted curve and black curve corresponded to rate of hydrogen evolution reaction (HER) and rate of the CO<sub>2</sub>-ERR respectively. The gap between these lines represents the rate of products. The result shows that, in 0.1 M KHCO<sub>3</sub>, the gap observed in CuNiSn/CS<sub>30</sub> (Fig.10b), CuSn/CS<sub>30</sub> (Fig.10c) and Cu/CS<sub>30</sub> (Fig.10f) was larger than that of CuNi/CS<sub>30</sub>, NiSn/CS<sub>30</sub> and Ni/CS<sub>30</sub>. It suggests that CuNiSn/CS<sub>30</sub>, CuSn/CS<sub>30</sub> and Cu/CS<sub>30</sub> had a higher catalytic activity than CuNi/CS<sub>30</sub>, NiSn/CS<sub>30</sub> and Ni/CS<sub>30</sub> in 0.1 M KHCO<sub>3</sub> over studied potentials.

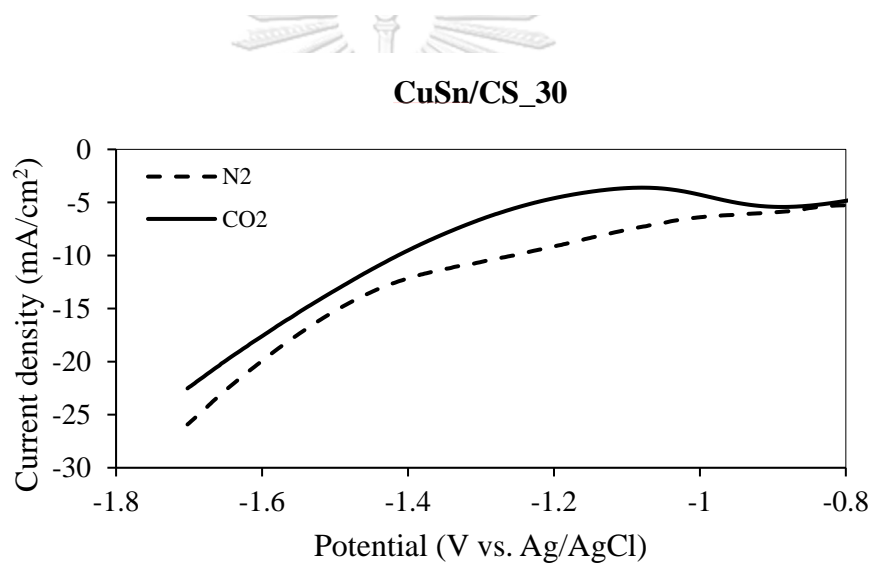
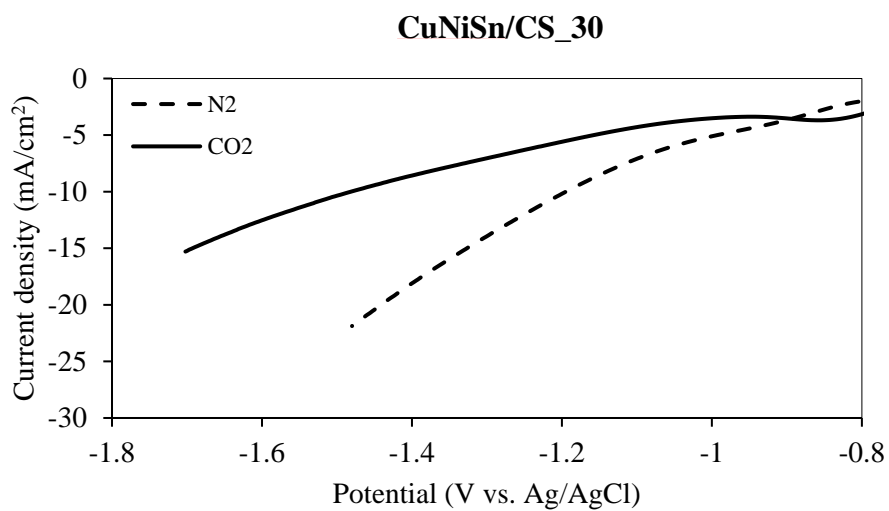
In addition, For the CuNiSn/CS<sub>30</sub>, CuSn/CS<sub>30</sub> and Cu/CS<sub>30</sub> electrocatalysts behaved similarly in the presence of CO<sub>2</sub>, the cathodic current was decreased at potentials less than -0.9 V vs. Ag/AgCl, which is attributed to the inhibition of HER due to the adsorption of species derived from CO<sub>2</sub> reduction such as CO and formates [19], [22], [30]. These results show that CO<sub>2</sub> is effectively reduced to adsorbed species on all the catalyst surfaces.

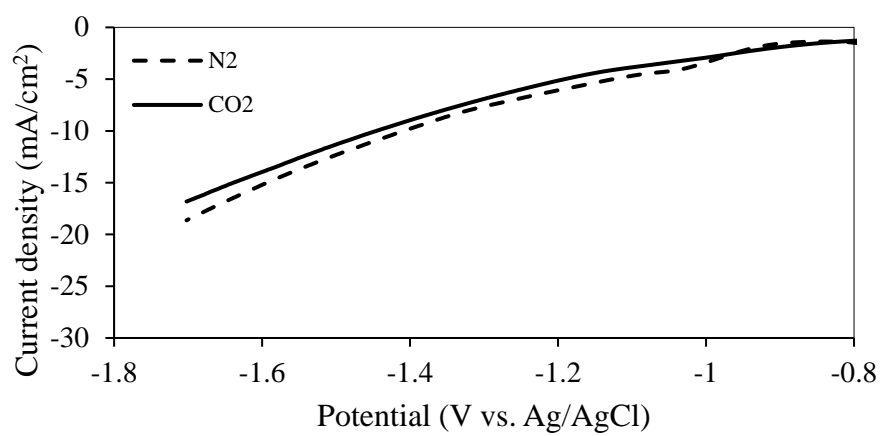
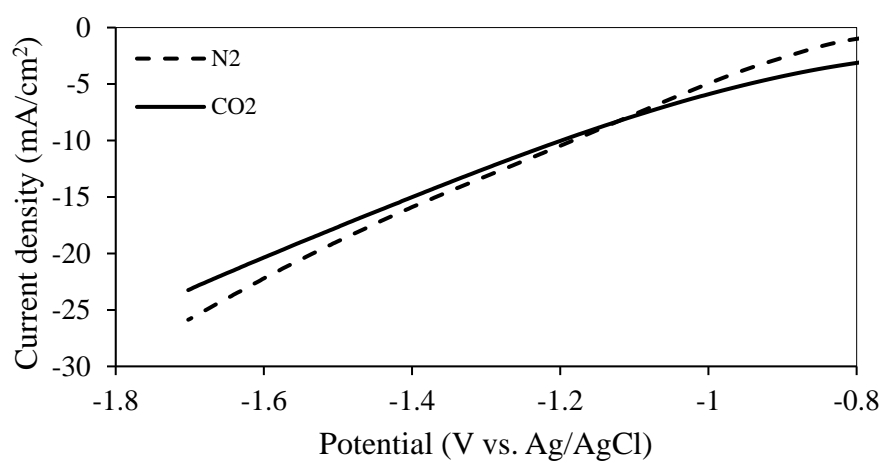
จุฬาลงกรณ์มหาวิทยาลัย

**Carbon fabric (CS)**







**CuNi/CS\_30****NiSn/CS\_30**

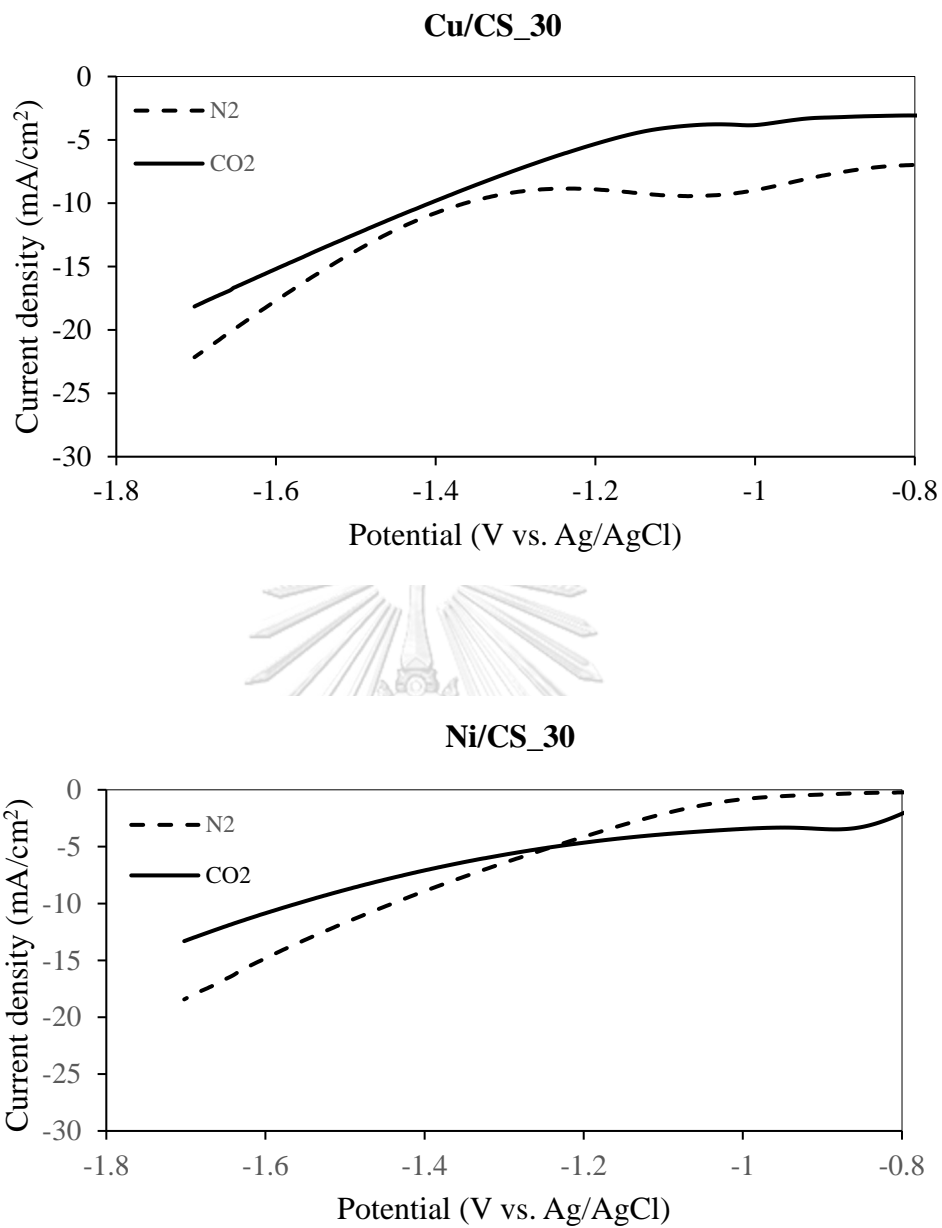


Figure 10. LSV curves of a) Carbon fabric b) CuNiSn/CS<sub>30</sub> c) CuSn/CS<sub>30</sub> and d) CuNi/CS<sub>30</sub> e) NiSn/CS<sub>30</sub> f) Cu/CS<sub>30</sub> and g) Ni/CS<sub>30</sub> in N<sub>2</sub> and CO<sub>2</sub> saturated solutions (0.1M KHCO<sub>3</sub>) with a scan rate 100 mV/s.

#### 4.2.4 Activity test of electrocatalyst for the CO<sub>2</sub>-ERR

To compare the activity of tri, bi and monometallic alloy electrocatalysts, all the electrocatalysts were tested via the CO<sub>2</sub>-ERR at -1.6 V vs. Ag/AgCl for 150 minutes in CO<sub>2</sub> saturated 0.1 M KHCO<sub>3</sub> as shown in Table 6. The obtained gas product included H<sub>2</sub> as a main product. When CO<sub>2</sub>-ERR was performed on Cu/CS<sub>30</sub>, Ni/CS<sub>30</sub> (monometallic) and CuSn/CS<sub>30</sub>, CuNi/CS<sub>30</sub> and NiSn/CS<sub>30</sub> (bi-metallic), Faradaic Efficiency (FE) of H<sub>2</sub> production was over 100% and produced a high rate of H<sub>2</sub> production in 0.1 M KHCO<sub>3</sub> at -1.6 V vs. Ag/AgCl. Because Cu is the only metal that can be used to produce hydrocarbons and oxygenate[20] but Cu promotes high hydrogen coverage at voltages more negative than -0.8 V [39] and Ni is regarded as increasing activity towards hydrogen evolution [39].

For, the CuSn/CS<sub>30</sub> and Cu/CS<sub>30</sub> were able to provide gas products including CO and H<sub>2</sub>, while other electrocatalysts produced only H<sub>2</sub>. The result was consistent with the research of Saad Sarfraz [31], indicating a selective and stable electrocatalyst for the efficient and selective conversion of CO<sub>2</sub> to CO over a large potential range using non-noble metals such as Cu and Sn. The Cu-Sn bimetallic electrocatalyst creates a surface that prevents adsorbed H\*, leading to enhanced CO production, whereas the pure monometallic surfaces (Cu) fail to selectively reduce CO<sub>2</sub>. Thus, most of CO on CuSn/CS<sub>30</sub> and Cu/CS<sub>30</sub> can be easily converted into formate, C<sub>2</sub> product and C<sub>3</sub> product.

Moreover, the CuNiSn/CS<sub>30</sub> (tri-metallic) showed the decrease in the H<sub>2</sub> production, subsequently H<sub>2</sub> evolution was greatly decreased to a FE of 33%, compared to bi-metallic and mono-metallic electrocatalyst, probably because they have multiple active sites able to function during the reaction.

Additionally, the liquid products from NMR analysis showed that formate, ethylene glycol, acetone, and ethanol were produced from the CO<sub>2</sub>-ERR. It was indicated that copper was the active metal for the formation of formate, which could be observed from CuSn/CS<sub>30</sub> and Cu/CS<sub>30</sub>. Tin could help increase the rates of formations of formate (CuSn/CS<sub>30</sub> and Cu/CS<sub>30</sub>) and ethanol (NiSn/CS<sub>30</sub> and Ni/CS<sub>30</sub>). Moreover, nickel was the active metal for the formation of ethylene glycol,

acetone, and ethanol. For CuNiSn/C\_30, the main two products were ethanol and ethylene glycol, respectively.

For reaction pathway, we suggested that Cu-based catalysts have a proton coupled electron transfer to an adsorbed intermediate like \*OCHO to form formate. For Ni-based catalysts, it is believed that the intermediate \*OCHO can transform to \*CHO, followed by CO insertion to form ethanol and ethylene glycol; additionally, \*CHO with CO coupling can produce acetone. Although the %FEs of liquid products were relatively low, the present study's objective was to demonstrate the feasibility of the concept used for the synthesized electrocatalysts. In our next study, to improve the reaction performance, the stoichiometry of deposited metals and the influences of electrolytes, including types, pH, and concentrations need to be studied.

Table 6. The catalytic activity of tri, bi and monometallic alloy electrocatalyst of CO<sub>2</sub>-ERR

Electrocatalyst	Rate of gas products (μmol/min)		Faradic Efficiency (FE)		Rate of liquid products (μmol/min)				Faradic Efficiency (FE)			
	H <sub>2</sub>	CO	H <sub>2</sub>	CO	Formate	Ethylene glycol	Acetone	Ethanol	Formate	Ethylene glycol	Acetone	Ethanol
1.CuNiSn/CS_30	3.50	-	33%	-	0.0030	0.0140	0.0030	0.0140	0.07%	1.38%	0.57%	1.71%
2.CuSn/CS_30	11.80	1.30	100%	13%	0.1030	0.0250	0.0050	0.0240	1.81%	2.17%	0.76%	2.50%
3.CuNi/CS_30	10.90	-	100%	-	0.0400	0.0590	0.0080	0.0250	0.74%	5.78%	1.31%	2.94%
4.NiSn/CS_30	9.90	-	100%	-	0.0009	0.0130	0.0100	0.0200	0.02%	1.22%	1.49%	2.38%
5.Cu/CS_30	9.50	0.02	100%	0.2%	0.0920	0.0300	0.0170	0.0240	1.41%	2.28%	2.09%	2.22%
6.Ni/CS_30	13.40	-	100%	-	0.0090	0.0130	0.0100	0.0050	0.16%	1.07%	1.33%	0.48%

**Part III.** To investigate the activity and stability of electrocatalysts

#### 4.3 Stability of electrocatalysts

Finally, stability of electrocatalyst was studied using a constant potential at -1.6V vs. Ag/AgCl applied for CuNiSn/CS\_30, Cu/CS\_30 and Ni/CS\_30 electrocatalyst. Figure 11 showed that CuNiSn/CS\_30 remained stable even after 1800 seconds. During the reaction, the current density for monometallic Cu and Ni appeared to drop quite quickly and eventually approach a very low current density. It was indicated that the synergistic effect of copper, nickel, and tin could improve the catalyst stability. Therefore, the conclusion can be drawn that CuNiSn/C\_30 provided high stability and strong resistance toward CO<sub>2</sub>-ERR.

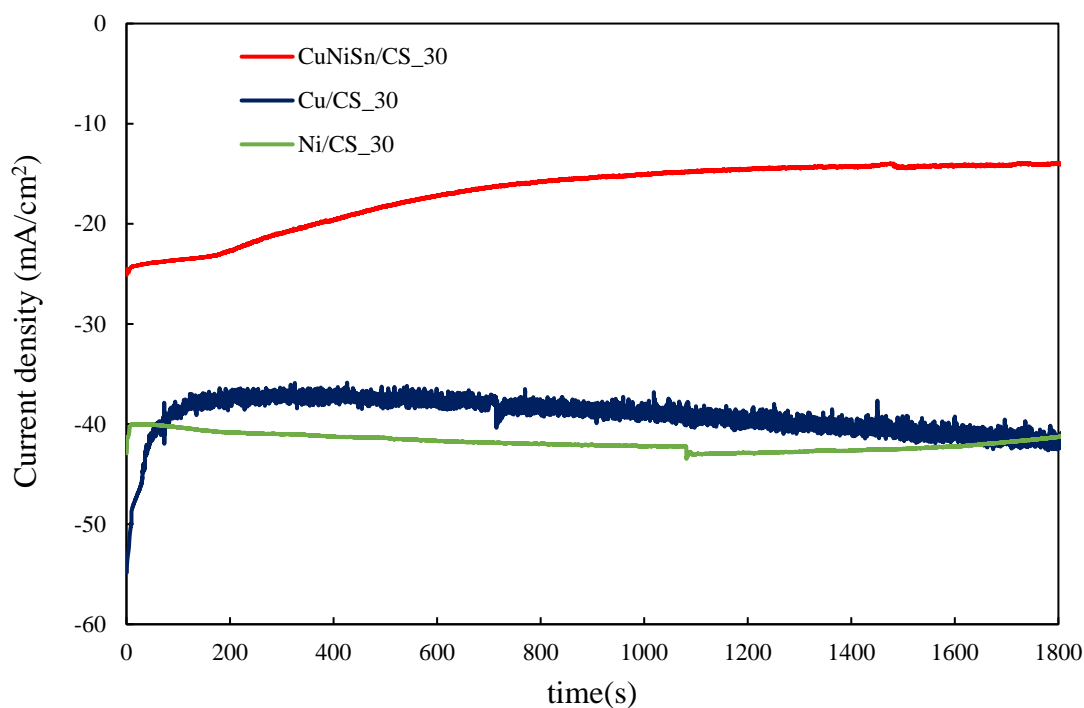


Figure 11. Electrochemical stability of electrodes in 0.1M KHCO<sub>3</sub>

## CHAPTER V

### CONCLUSIONS

#### 5.1 Conclusion

The tri, bi and mono metallic alloy electrocatalysts were prepared by electroless deposition method. As-deposited tri, bi and mono metallic alloy electrocatalyst supported on carbon fabric by palladium polymer ink was used for CO<sub>2</sub>-ERR. For the effect of electroless deposition time for CuNiSn electrocatalysts, the structure of CuNiSn/CS<sub>15</sub>, CuNiSn/CS<sub>30</sub> and CuNiSn/CS<sub>45</sub> obtained from electroless deposition showed no significant difference for all samples based on the XRD pattern. Thus, it can be concluded that the deposition time had no effect on the crystalline structure of all catalysts. In addition, the evaluation of the ability of the CO<sub>2</sub>-ERR on trimetallic alloy electrocatalyst at different times was investigated using linear sweep voltammetry (LSV). The result showed that CuNiSn/CS<sub>30</sub> had a higher catalytic activity than CuNiSn/CS<sub>45</sub> and CuNiSn/CS<sub>15</sub> respectively.

Mono-metallic and bi-metallic alloy electrocatalyst displayed different activities toward the H<sub>2</sub> evolution reaction, which occurs during CO<sub>2</sub> reduction in aqueous electrolytes. Despite these apparent differences, a significant reduction in the current developed in the H<sub>2</sub> evolution region was observed for all the electrocatalysts, demonstrating the adsorption of species derived from CO<sub>2</sub> reduction on all the electrode surfaces. For, CuSn/CS<sub>30</sub> and Cu/CS<sub>30</sub> was found to be able to provide gas products with CO other than H<sub>2</sub> compared to other electrocatalysts. Thus, most of CO on CuSn/CS<sub>30</sub> and Cu/CS<sub>30</sub> can be easily converted into formate, C<sub>2</sub> product and C<sub>3</sub> product. Moreover, the trimetallic electrode (CuNiSn/CS) provides better reaction performance than monometallic and bimetallic electrodes and this is supported by its lower FE for H<sub>2</sub> production, suggesting that it has multiple active sites able to function during the reaction.

The liquid products including formate, ethylene glycol, acetone, and ethanol were produced from the CO<sub>2</sub>-ERR. Copper was the active metal for the formation of formate. Tin could help increase the rates of formations of formate and ethanol. Nickel was the active metal for the formation of ethylene glycol, acetone, and ethanol.

Moreover, different intermediates over Cu-based and Ni-based catalysts were proposed.

### 5.2 Recommendations

1. The electroless bath composition need to be studied. For instance,  $\text{NiSO}_4:\text{CuSO}_4$  need to be varied to obtain the optimum ratio
2. The influences of electrolytes, including types, pH, and concentrations need to be studied.
3. The applied potential may need to be varied less than  $-1.6\text{ V}$  vs Ag/AgCl





## REFERENCES

[26]



จุฬาลงกรณ์มหาวิทยาลัย  
**CHULALONGKORN UNIVERSITY**

- [1] O. S. Bushuyev *et al.*, “What Should We Make with CO<sub>2</sub> and How Can We Make It?,” *Joule*, vol. 2, no. 5, pp. 825–832, May 2018, doi: 10.1016/j.joule.2017.09.003.
- [2] M. Mikkelsen, M. Jørgensen, and F. C. Krebs, “The teraton challenge. A review of fixation and transformation of carbon dioxide,” *Energy Environ. Sci.*, vol. 3, no. 1, pp. 43–81, 2010, doi: 10.1039/B912904A.
- [3] A. Sanna, M. Uibu, G. Caramanna, R. Kuusik, and M. M. Maroto-Valer, “A review of mineral carbonation technologies to sequester CO<sub>2</sub>,” *Chem. Soc. Rev.*, vol. 43, no. 23, pp. 8049–8080, 2014, doi: 10.1039/C4CS00035H.
- [4] Y. A. Daza, R. A. Kent, M. M. Yung, and J. N. Kuhn, “Carbon Dioxide Conversion by Reverse Water–Gas Shift Chemical Looping on Perovskite-Type Oxides,” *Ind. Eng. Chem. Res.*, vol. 53, no. 14, pp. 5828–5837, Apr. 2014, doi: 10.1021/ie5002185.
- [5] N. Uemoto, M. Furukawa, I. Tateishi, H. Katsumata, and S. Kaneco, “Electrochemical Carbon Dioxide Reduction in Methanol at Cu and Cu<sub>2</sub>O-Deposited Carbon Black Electrodes,” *ChemEngineering*, vol. 3, no. 1, p. 15, Feb. 2019, doi: 10.3390/chemengineering3010015.
- [6] P. K. Jiwanti, S. Sultana, W. P. Wicaksono, and Y. Einaga, “Metal modified carbon-based electrode for CO<sub>2</sub> electrochemical reduction: A review,” *Journal of Electroanalytical Chemistry*, vol. 898, p. 115634, Oct. 2021, doi: 10.1016/j.jelechem.2021.115634.
- [7] J. N. Balaraju, “Electroless Ni–P composite coatings,” p. 10.
- [8] S. Pourhosseini, H. Beygi, and S. A. Sajjadi, “Effect of metal coating of reinforcements on the microstructure and mechanical properties of Al–Al<sub>2</sub>O<sub>3</sub> nanocomposites,” *Materials Science and Technology*, vol. 34, no. 2, pp. 145–152, Jan. 2018, doi: 10.1080/02670836.2017.1366708.
- [9] S. Pérez-Rodríguez, E. Pastor, and M. J. Lázaro, “Noble metal-free catalysts supported on carbon for CO<sub>2</sub> electrochemical reduction,” *Journal of CO<sub>2</sub> Utilization*, vol. 18, pp. 41–52, Mar. 2017, doi: 10.1016/j.jcou.2017.01.010.
- [10] M. Azuma, K. Hashimoto, M. Hiramoto, M. Watanabe, and T. Sakata, “Carbon dioxide reduction at low temperature on various metal electrodes,” *Journal of Electroanalytical Chemistry and Interfacial Electrochemistry*, vol. 260, no. 2, pp. 441–445, Mar. 1989, doi: 10.1016/0022-0728(89)87158-X.
- [11] W. Lv, R. Zhang, P. Gao, and L. Lei, “Studies on the faradaic efficiency for electrochemical reduction of carbon dioxide to formate on tin electrode,” *Journal of Power Sources*, vol. 253, pp. 276–281, May 2014, doi: 10.1016/j.jpowsour.2013.12.063.
- [12] Y. Chen and M. W. Kanan, “Tin Oxide Dependence of the CO<sub>2</sub> Reduction Efficiency on Tin Electrodes and Enhanced Activity for Tin/Tin Oxide Thin-Film Catalysts,” *J. Am. Chem. Soc.*, vol. 134, no. 4, pp. 1986–1989, Feb. 2012, doi: 10.1021/ja2108799.
- [13] K. Ye *et al.*, “Synergy effects on Sn–Cu alloy catalyst for efficient CO<sub>2</sub> electroreduction to formate with high mass activity,” *Science Bulletin*, vol. 65, no. 9, pp. 711–719, May 2020, doi: 10.1016/j.scib.2020.01.020.
- [14] X. Bai *et al.*, “Exclusive Formation of Formic Acid from CO<sub>2</sub> Electroreduction by a Tunable Pd–Sn Alloy,” *Angew. Chem. Int. Ed.*, vol. 56, no. 40, pp. 12219–12223, Sep. 2017, doi: 10.1002/anie.201707098.

- [15] W.-N. Wang, J. Soulis, Y. J. Yang, and P. Biswas, "Comparison of CO<sub>2</sub> Photoreduction Systems: A Review," *Aerosol Air Qual. Res.*, vol. 14, no. 2, pp. 533–549, 2014, doi: 10.4209/aaqr.2013.09.0283.
- [16] W. Luc *et al.*, "Ag–Sn Bimetallic Catalyst with a Core–Shell Structure for CO<sub>2</sub> Reduction," *J. Am. Chem. Soc.*, vol. 139, no. 5, pp. 1885–1893, Feb. 2017, doi: 10.1021/jacs.6b10435.
- [17] X. Zhang *et al.*, "Atomic nickel cluster decorated defect-rich copper for enhanced C<sub>2</sub> product selectivity in electrocatalytic CO<sub>2</sub> reduction," *Applied Catalysis B: Environmental*, vol. 291, p. 120030, Aug. 2021, doi: 10.1016/j.apcatb.2021.120030.
- [18] T. M. Suzuki *et al.*, "Electrochemical CO<sub>2</sub> reduction over nanoparticles derived from an oxidized Cu–Ni intermetallic alloy," *Chem. Commun.*, vol. 56, no. 95, pp. 15008–15011, 2020, doi: 10.1039/D0CC06130A.
- [19] T.-V. Phuc, J.-S. Chung, and S.-H. Hur, "Highly CO Selective Trimetallic Metal–Organic Framework Electrocatalyst for the Electrochemical Reduction of CO<sub>2</sub>," *Catalysts*, vol. 11, no. 5, p. 537, Apr. 2021, doi: 10.3390/catal11050537.
- [20] C. Chen, J. F. Khosrowabadi Kotyk, and S. W. Sheehan, "Progress toward Commercial Application of Electrochemical Carbon Dioxide Reduction," *Chem*, vol. 4, no. 11, pp. 2571–2586, Nov. 2018, doi: 10.1016/j.chempr.2018.08.019.
- [21] R. J. Dixit and C. B. Majumder, "CO<sub>2</sub> capture and electro-conversion into valuable organic products: A batch and continuous study," *Journal of CO<sub>2</sub> Utilization*, vol. 26, pp. 80–92, Jul. 2018, doi: 10.1016/j.jcou.2018.04.027.
- [22] J. Qiao, Y. Liu, and J. Zhang, Eds., *Electrochemical Reduction of Carbon Dioxide: Fundamentals and Technologies*. CRC Press, 2016. doi: 10.1201/b20177.
- [23] Y. Jia, F. Li, K. Fan, and L. Sun, "Cu-based bimetallic electrocatalysts for CO<sub>2</sub> reduction," *Advanced Powder Materials*, p. 100012, Nov. 2021, doi: 10.1016/j.apmate.2021.10.003.
- [24] S. Garg *et al.*, "Advances and challenges in electrochemical CO<sub>2</sub> reduction processes: an engineering and design perspective looking beyond new catalyst materials," *J. Mater. Chem. A*, vol. 8, no. 4, pp. 1511–1544, 2020, doi: 10.1039/C9TA13298H.
- [25] G. Wang *et al.*, "Electrocatalysis for CO<sub>2</sub> conversion: from fundamentals to value-added products," *Chem. Soc. Rev.*, vol. 50, no. 8, pp. 4993–5061, 2021, doi: 10.1039/D0CS00071J.
- [26] K. P. Kuhl, E. R. Cave, D. N. Abram, and T. F. Jaramillo, "New insights into the electrochemical reduction of carbon dioxide on metallic copper surfaces," *Energy Environ. Sci.*, vol. 5, no. 5, p. 7050, 2012, doi: 10.1039/c2ee21234j.
- [27] D. Ren, J. Fong, and B. S. Yeo, "The effects of currents and potentials on the selectivities of copper toward carbon dioxide electroreduction," *Nat Commun*, vol. 9, no. 1, p. 925, Dec. 2018, doi: 10.1038/s41467-018-03286-w.
- [28] M. Moradi, B. Gerami Shirazi, A. Sadeghi, and S. Seidi, "Electroless plating of Sn/Cu/Zn triple layer on AA6082 aluminum alloy," *International Journal of Lightweight Materials and Manufacture*, vol. 5, no. 1, pp. 1–10, Mar. 2022, doi: 10.1016/j.ijlmm.2021.08.002.
- [29] K. P. Kuhl, T. Hatsukade, E. R. Cave, D. N. Abram, J. Kibsgaard, and T. F. Jaramillo, "Electrocatalytic Conversion of Carbon Dioxide to Methane and

- Methanol on Transition Metal Surfaces,” *J. Am. Chem. Soc.*, vol. 136, no. 40, pp. 14107–14113, Oct. 2014, doi: 10.1021/ja505791r.
- [30] J. T. Feaster *et al.*, “Understanding Selectivity for the Electrochemical Reduction of Carbon Dioxide to Formic Acid and Carbon Monoxide on Metal Electrodes,” *ACS Catal.*, vol. 7, no. 7, pp. 4822–4827, Jul. 2017, doi: 10.1021/acscatal.7b00687.
- [31] S. Sarfraz, A. T. Garcia-Esparza, A. Jedidi, L. Cavallo, and K. Takanabe, “Cu–Sn Bimetallic Catalyst for Selective Aqueous Electroreduction of CO<sub>2</sub> to CO,” *ACS Catal.*, vol. 6, no. 5, pp. 2842–2851, May 2016, doi: 10.1021/acscatal.6b00269.
- [32] F. Liao, X. Han, Y. Zhang, C. Xu, and H. Chen, “Carbon fabrics coated with nickel film through alkaline electroless plating technique,” *Materials Letters*, vol. 205, pp. 165–168, Oct. 2017, doi: 10.1016/j.matlet.2017.06.087.
- [33] R. Y. Mahmood and A. A. Kareem, “Characteristics of electroless copper plating on modified carbon fiber,” Rhodes, Greece, 2020, p. 050022. doi: 10.1063/5.0027392.
- [34] K. Muhammet, A. Ahmet, and A. Hatem, “PREPARATION OF TIN@CARBON FIBER COMPOSITES BY ELECTROLESS DEPOSITION,” p. 5, 2016.
- [35] W. Chaitree and E. E. Kalu, “Co-Ni-Mo as a Non-Noble Metal Electrocatalyst for Ethanol Electro-Oxidation,” *J. Electrochem. Soc.*, vol. 166, no. 10, pp. H392–H403, 2019, doi: 10.1149/2.0041910jes.
- [36] S. Ghosh, “Electroless copper deposition: A critical review,” *Thin Solid Films*, vol. 669, pp. 641–658, Jan. 2019, doi: 10.1016/j.tsf.2018.11.016.
- [37] G. Dai, S. Wu, and X. Huang, “Preparation process for high-entropy alloy coatings based on electroless plating and thermal diffusion,” *Journal of Alloys and Compounds*, vol. 902, p. 163736, May 2022, doi: 10.1016/j.jallcom.2022.163736.
- [38] S. M. Badawy, R. A. El Khashab, and A. A. Nayl, “Synthesis, Characterization and Catalytic Activity of Cu/Cu<sub>2</sub>O Nanoparticles Prepared in Aqueous Medium,” *Bull. Chem. React. Eng. Catal.*, vol. 10, no. 2, pp. 169–174, Jul. 2015, doi: 10.9767/brec.10.2.7984.169-174.
- [39] Hannah L.A. Dickinson and M. D. Symes, “Recent progress in CO<sub>2</sub> reduction using bimetallic electrodes containing copper,” *Electrochemistry Communications*, vol. 135, p. 107212, Feb. 2022, doi: 10.1016/j.elecom.2022.107212.

## VITA

**NAME** Atikom Hongmeuan

**DATE OF BIRTH** 07 April 1998

**PLACE OF BIRTH** Bangkok, Thailand

**INSTITUTIONS  
ATTENDED** B.Sc.Industrial Chemistry  
King Mongkut's Institute of Technology Ladkrabang  
(KMITL)

**HOME ADDRESS** 141/1 , Bang Khun Kong , Bang Kruai , Nonthaburi 11130



จุฬาลงกรณ์มหาวิทยาลัย  
CHULALONGKORN UNIVERSITY